JPn Neuroscience

The Journal of Physiology

*J Physiol* 594.22 (2016) pp 6679–6699



# Inhibitory masking controls the threshold sensitivity of retinal ganglion cells

Feng Pan[1,5], Abduqodir Toychiev[1], Yi Zhang[2], Tamas Atlasz[3], Hariharasubramanian Ramakrishnan[1], Kaushambi Roy[1], Béla Völgyi[3,4], Abram Akopian[1] and Stewart A. Bloomfield[1]

[1]*Department of Biological and Vision Sciences, State University of New York College of Optometry, New York, NY, USA*
[2]*F. M. Kirby Neurobiology Center, Boston Children's Hospital, Harvard Medical School, Boston, MA, USA*
[3]*Department of Sport Biology, Janos Szentagothai Research Center, University of Pécs, Pécs, Hungary*
[4]*Department of Experimental Zoology and Neurobiology, Janos Szentagothai Research Center, University of Pécs, Pécs, Hungary*
[5]*Current address: School of Optometry, The Hong Kong Polytechnic University, Hung Hom, Kowloon, Hong Kong*

**Key points**

- Retinal ganglion cells (RGCs) in dark-adapted retinas show a range of threshold sensitivities spanning ~3 log units of illuminance.
- Here, we show that the different threshold sensitivities of RGCs reflect an inhibitory mechanism that masks inputs from certain rod pathways.
- The masking inhibition is subserved by $GABA_C$ receptors, probably on bipolar cell axon terminals.
- The GABAergic masking inhibition appears independent of dopaminergic circuitry that has been shown also to affect RGC sensitivity.
- The results indicate a novel mechanism whereby inhibition controls the sensitivity of different cohorts of RGCs. This can limit and thereby ensure that appropriate signals are carried centrally in scotopic conditions when sensitivity rather than acuity is crucial.

**Abstract** The responses of rod photoreceptors, which subserve dim light vision, are carried through the retina by three independent pathways. These pathways carry signals with largely different sensitivities. Retinal ganglion cells (RGCs), the output neurons of the retina, show a wide range of sensitivities in the same dark-adapted conditions, suggesting a divergence of the rod pathways. However, this organization is not supported by the known synaptic morphology of the retina. Here, we tested an alternative idea that the rod pathways converge onto single RGCs, but inhibitory circuits selectively mask signals so that one pathway predominates. Indeed, we found that application of GABA receptor blockers increased the sensitivity of most RGCs by unmasking rod signals, which were suppressed. Our results indicate that inhibition controls the threshold responses of RGCs under dim ambient light. This mechanism can ensure that appropriate signals cross the bottleneck of the optic nerve in changing stimulus conditions.

(Received 10 February 2016; accepted after revision 23 June 2016; first published online 28 June 2016)
**Corresponding author** S. A. Bloomfield: Department of Biological and Vision Science, SUNY College of Optometry, 33 West 42nd Street, New York, NY 10036, USA. Email: sbloomfield@sunyopt.edu

**Abbreviations** AC, amacrine cell; BC, bipolar cell; HS, high sensitivity; IS, intermediate sensitivity; LIS, low-intermediate sensitivity; LS, low sensitivity; MEA, multielectrode array; PTX, picrotoxin; RGC, retinal ganglion cell; SR-95531, gabazine; TPMPA, 1,2,5,6-tetrahydropyridin-4-yl-methylphosphinic acid.

## Introduction

The transition between rod and cone photoreceptor signalling enables the retina to respond over the ~10 log units of ambient luminance encountered between night and day. Rods and cones are presynaptic to different bipolar cells, thereby segregating signals into parallel


DOI: 10.1113/JP272267

streams (Dowling & Boycott, 1966; Boycott & Kolb, 1973; Ghosh *et al.* 2004). Whereas >10 subtypes of bipolar cell (BCs) are postsynaptic to cones, providing a number of vertical pathways to the output retinal ganglion cells (RGCs), the radial propagation of scotopic or rod signals is limited to three distinct pathways (Raviola & Gilula, 1973; Famiglietti & Kolb, 1975; Nelson, 1977; Strettoi *et al.* 1990; Boycott & Wässle, 1991; Euler & Wässle, 1995; Schneeweis & Schnapf, 1995; Soucy *et al.* 1998; Hack *et al.* 1999; Tsukamoto *et al.* 2001; Fyk-Kolodziej *et al.* 2003; Li *et al.* 2004; Fig. 1). Both human and animal studies support a pathway segregation whereby the primary rod pathway transmits the most sensitive signals, while the secondary pathway carries rod signals with ∼1 log unit less sensitivity (Blakemore & Rushton, 1965*a*,*b*; Balkema & Pinto, 1982; Conner, 1982; Müller *et al.* 1988; DeVries & Baylor, 1995; Deans *et al.* 2002; Völgyi *et al.* 2004). The third rod pathway appears to carry the least sensitive rod signals, generated in relatively brighter light conditions, such as during dusk or dawn (Tsukamoto *et al.* 2001; Völgyi *et al.* 2004; Pang *et al.* 2010).

Interestingly, it has been found that RGCs display a wide range of threshold sensitivities in the same dark-adapted conditions, suggesting a division of labour between the three rod pathways whereby they innervate different RGC subtypes (Balkema & Pinto, 1982; Stone & Pinto, 1993; Lee *et al.* 1997; Deans *et al.* 2002; Völgyi *et al.* 2004). Such segregated targeting of the rod pathways has important implications concerning the rod circuitry in the retina. For example, lack of primary pathway signalling to certain RGCs would require certain subtypes of ON cone BCs not to form gap junctions with the AII amacrine cells (ACs; Fig. 1). Likewise, the secondary pathway could avoid innervating certain RGCs only if not all cones are coupled to rods, whereby only a limited number of ON cone BC subtypes carried rod signals (Fig. 1). However, such selectivity in the electrical coupling of photoreceptors has not been seen (Raviola & Gilula, 1973; Schneeweis & Schnapf, 1995; Tsukamoto *et al.* 2001) and most, if not all, cone BCs form gap junctions with AII ACs (Cohen & Sterling, 1990*b*; Tsukamoto *et al.* 2001; Veruki & Hartveit, 2002; Petrides & Trexler, 2008).

An alternative explanation for the apparent segregation of the rod pathways' signalling to RGCs is that certain scotopic inputs are masked because of an intrinsic RGC mechanism (Beaudoin *et al.* 2008) or selective inhibition either directly on or presynaptic to RGCs (Dowling & Boycott, 1966). This idea is supported by the findings that subthreshold current and spike responses of individual RGCs can display different threshold sensitivities (Pang *et al.* 2003; Beaudoin *et al.* 2008).

Here, we tested the hypothesis that the wide range of RGC threshold sensitivities reflects inhibition that selectively masks the different signals carried by the multiple rod pathways. Consistent with this idea, we found that application of GABAergic blockers resulted in a robust shift in the threshold and intensity–response functions of most RGCs to more sensitive levels. The inhibition

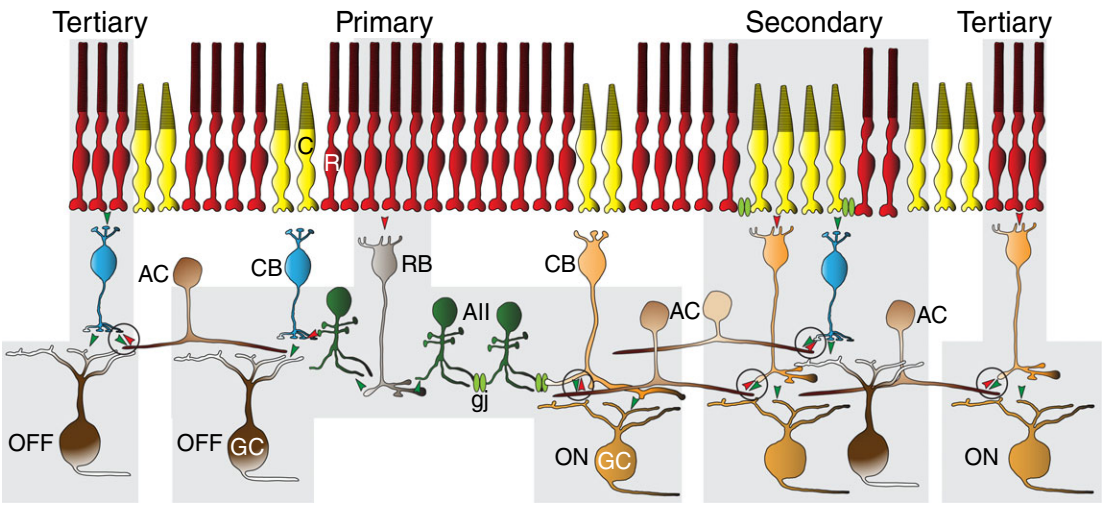


**Figure 1. The three rod pathways in the mammalian retina**
In the primary pathway, rods (R) transfer signals to postsynaptic rod bipolar cells (BCs; RB) and, in turn, to AII amacrine cells (ACs). The AII cells form gap junctions (gj) with ON cone BCs (CB) and inhibitory glycinergic synapses with OFF cone BCs, which pass rod signals to ON and OFF retinal gangion cells, respectively. The secondary rod pathway is formed by gap junctions between rods and cones (C), in which rod signals are passed directly to cones and then to cone BCs. The tertiary rod pathway is formed by rod synapses onto a unique type of OFF BC and possibly also to a type of ON cone BC, thereby forming complimentary ON and OFF circuits. The feedback inhibitory synapses from ACs to BC axon terminals proposed to be responsible for selective masking rod pathway signals are encircled. [Colour figure can be viewed at wileyonlinelibrary.com]

was derived mainly from activation of $GABA_C$ receptors presynaptic to RGCs in the inner retina. Overall, our findings reveal an inhibitory masking mechanism, which can regulate the threshold sensitivity of different cohorts of RGCs. This novel mechanism can limit the signals sent centrally so as to ensure the efficient transfer of appropriate visual information across the optic nerve bottleneck in different adaptation conditions.

## Methods

### Ethical approval

All animal procedures were approved by the Institutional Animal Care and Use Committee of the SUNY College of Optometry and comply with the *Guide for the Care and Use of Laboratory Animals* published by the National Institutes of Health.

### Flattened retina–sclera preparation

Adult (postnatal day 42–90) C57BL/C57BL:129 [wild-type (WT), $n = 51$], $Cx36^{-/-}$ ($n = 10$) and Kcng4-YFP ($n = 8$) mice (Deans *et al.* 2002; Duan *et al.* 2015) were used in the study. Animals were maintained in a 12 h–12 h day–night cycle, and all experiments were performed during daylight hours. The mice were anaesthetized deeply with an intraperitoneal injection of ketamine (Vedno, St. Joseph, MO, USA) and xylazine (Akorn, Decatur, IL, USA) [80 and 10 mg (kg body weight)$^{-1}$, respectively], and lidocaine hydrochloride (20 mg ml$^{-1}$, Sigma-Aldrich, St. Louis, MO, USA) was applied locally to the eyelids and surrounding tissue. Eyes were removed under dim red illumination and hemisected anterior to the ora serrata. Anterior optics and the vitreous humor were removed, and the resultant retina–eyecup with sclera attached, either whole or in sections, was placed in a superfusion chamber. For whole retina–eyecups, several radial incisions were made peripherally, allowing the eyecup to be flattened. For patch-clamp recordings, retina–eyecups were dissected into four equal quadrants and attached to a modified translucent Millicell filter ring (Millipore, Bedford, MA, USA). The flattened retina–eyecups were superfused with oxygenated mammalian Ringer solution, pH 7.4, at 32°C (Bloomfield & Miller, 1982). Anaesthetized animals were killed by cervical dislocation immediately after the enucleations.

### Light stimulation

A green (525 nm) light-emitting diode delivered uniform full-field visual stimuli on the surface of the retina. The intensity of the square-wave light stimuli was calibrated with a portable radiometer/photometer (Ealing Electro-Optics, Holliston, MA, USA) and expressed in terms of the time-averaged rate of photoisomerizations per rod per second (Rh* per rod s$^{-1}$). Light intensities were calculated assuming an average rod density of 437,000 rods mm$^{-2}$ (Jeon *et al.* 1998) and quantum efficiency of 0.67 (Penn & Williams, 1984).

### Electrical recording

Extracellular recordings were obtained from RGCs in all retinal quadrants by using tungsten microelectrodes with resistances of 0.4–1.2 MΩ (Kation Scientific, Minneapolis, MN, USA) or a multielectrode array (MEA). For MEA experiments, retina–eyecups (37 WT and 10 $Cx36^{-/-}$ mice) were isolated, mounted on filter paper (8 $\mu$m pore size; Millipore) and placed RGC side down on the grid of a 60-channel electrode array (Multi Channel Systems, Reutlingen, Germany). Tungsten microelectrode recordings were made from whole retina–eyecups (six WT mice). Spike trains were recorded digitally at a sampling rate of 20 kHz with Axoscope software (Molecular Devices, Sunnyvale, CA, USA), with sorting by principal component analysis performed *post hoc* using Off-line Sorter (Plexon, Dallas, TX, USA) and NeuroExplorer (Nex Technologies, Littleton, MA, USA) software.

Whole-cell voltage- and current-clamp recordings were performed on RGCs in sections of the retina–eyecups (eight WT and eight Kcng4-YFP mice), using an Axopatch 200B amplifier connected to Digidata 1550A interface and pCLAMP 10 software (Molecular Devices). Cells were visualized with near infrared light (>775 nm) at ×40 magnification with a Nuvicon tube camera (Dage-MTI, Michigan City, IN, USA) and differential interference optics on a fixed-stage microscope (BX51WI; Olympus, Tokyo, Japan). Retina–eyecups were superfused at a rate of 1–1.5 ml min$^{-1}$ with a Ringer solution composed of (mM): 120 NaCl, 2.5 KCl, 25 $NaHCO_3$, 0.8 $Na_2HPO_4$, 0.1 $NaH2PO_4$, 1 $MgCl_2$, 2 $CaCl_2$ and 5 D-glucose. The bath solution was continuously bubbled with 95% $O_2$–5% $CO_2$ at temperature of ~32°C.

Whole-cell recordings were made with electrodes pulled to 5−7 MΩ resistance, with internal solutions consisting of (mM): 120 potassium gluconate, 12 KCl, 1 $MgCl_2$, 5 EGTA, 0.5 $CaCl_2$, 3 ATP, 0.2 GTP and 10 Hepes (pH adjusted to 7.4 with KOH). This internal solution was used in experiments where spiking was not blocked. In some experiments, to improve the space clamp and to block spiking, whole-cell EPSCs were recorded with an internal solution containing QX-314 (0.5 mM) and caesium methanosulfonate instead of potassium gluconate. The chloride equilibrium potential ($E_{Cl}$) with these internal solutions was approximately −63 mV. The excitatory and inhibitory current responses were isolated by holding the membrane potential approximately at the chloride or cation equilibrium/reversal potentials, −63 and −10 mV, respectively. Light-evoked EPSCs were filtered at 0.5 kHz and sampled at 2 kHz, digitized and stored directly on the

computer hard drive. Series resistance was compensated 70–80%. The liquid junction potential was estimated to be ∼15 mV and was subtracted from the holding membrane potential. Light-evoked spike activities were recorded in the current-clamp mode, with signals filtered at 2 kHz and sampled at 10 kHz.

### Pharmacology

Reagents were applied to the retina by switching from the control Ringer solution to one containing the drug. Reagents included picrotoxin (PTX) and SR-95531 (gabazine) obtained from Tocris (Bristol, UK); 1,2,5,6-tetrahydropyridin-4-yl-methylphosphinic acid (TPMPA), SCH 23390 and eticlopride obtained from Sigma-Aldrich (St Louis, MO, USA); and strychnine hydrochloride obtained from Sigma-Aldrich Research Biochemicals (Natick, MA, USA).

### Data analysis

Intensity–response profiles for individual cells were generated by tabulating spike counts or current amplitudes in 500 ms bins before, during and after the presentation of a stimulus of 500 ms duration with intensities varied over 5 log units. The number of light-evoked ON and OFF spikes of RGCs or current amplitudes were calculated by a subtraction of the background spike or current activity from those evoked by the light stimulus onset and offset, respectively. Cells were classified as sustained or transient, based on spike frequency parameters as described by Della Santina *et al.* (2013).

Averaged response data were then normalized and plotted against the intensity of the light stimuli with Origin software (OriginLab, Northampton, MA, USA). Data points were fitted by the classic Michaelis–Menten equation (Naka & Rushton, 1966; Baylor *et al.* 1974; Thibos & Werblin, 1978), as follows:

$$R = \frac{R_{\max} I^a}{I^a + \sigma^a}$$

Where $R$ is the measured response, $R_{\max}$ the maximal response, $I$ the stimulus intensity, $\sigma$ the light intensity that produces a response of $0.5R_{max}$, and $a$ is the Hill coefficient. Cells whose intensity–response functions showed a fit of $r^2 < 0.5$, probably because of deterioration of recording or adaptation changes during the stimulation series, were excluded from study. Response thresholds for individual cells were taken as 5% of the maximal spike frequency. Population histograms of response thresholds were fitted by non-linear regression using SigmaPlot software (Systat Software, San Jose, CA, USA). All data are reported as means ± SEM. Statistical significance ($P < 0.05$) was determined using Student's paired $t$ test.

## Results

### Segregation of mouse RGCs based on threshold sensitivity

Initial experiments were carried out to confirm earlier reports that RGCs show a wide range of threshold sensitivities in identical dark-adapted conditions (Balkema & Pinto, 1982; Lee *et al.* 1997; Deans *et al.* 2002; Völgyi *et al.* 2004). We recorded from ON ($n = 213$) and OFF cells ($n = 225$) in the ganglion cell layer of dark-adapted retinas either individually with tungsten electrodes or simultaneously using a MEA (Fig. 2*A*–*D*). As the ganglion cell layer of the mouse retina contains both RGCs and displaced ACs (Pérez De Sevilla Müller *et al.* 2007), it is plausible that our MEA recordings, made blindly, included both cell types. However, for tungsten electrode recordings we avoided somata with the very smallest diameters (<10 $\mu$m) to limit AC recordings. Overall, we found no statistically significant differences between data obtained using tungsten microelectrodes or the MEA. With the caveat that some may have been from displaced ACs in the ganglion cell layer, we will refer to all recordings as from RGCs.

Our sample included cells with a wide range of physiological spike activities, but they were classified broadly as ON transient ($n = 42$), ON sustained ($n = 171$), OFF transient ($n = 109$) and OFF sustained ($n = 116$), based on their light-evoked responses, following the model of Della Santina *et al.* (2013). Intensity–response profiles were created for each cell and fitted by single Michaelis–Menten functions, from which the average threshold sensitivities were computed (Fig. 2*E* and *F*). We found that RGCs in the same dark-adapted conditions showed a wide range of threshold sensitivities covering more than 3 log units (Fig. 2*G* and *H*). Although the population histograms for the threshold sensitivities of ON and OFF RGCs formed contiguous bands, each could be divided into four discrete components with non-linear regression curve fitting (Fig. 2*G* and *H*).

Following previously published nomenclature (Deans *et al.* 2002; Völgyi *et al.* 2004), the RGCs with the highest threshold ($n = 42$) were termed 'low sensitivity (LS)', which peaked at ∼20 Rh* per rod $s^{-1}$, corresponding to the threshold sensitivity of cone photoreceptors. This category includes both ON and OFF transient ($n = 5$) and ON and OFF sustained RGCs ($n = 37$). In contrast, the other three groups of RGCs, termed 'high sensitivity (HS)' (ON and OFF transient, $n = 14$; ON and OFF sustained, $n = 56$), 'intermediate sensitivity (IS)' (ON and OFF transient, $n = 62$; ON and OFF sustained, $n = 110$) and 'low-intermediate sensitivity (LIS)' (ON and OFF transient, $n = 70$; ON and OFF sustained, $n = 84$) responded within the scotopic intensity range and displayed threshold sensitivities of approximately 3, 2

and 1 log units, respectively, higher than that of LS cells (Fig. 2*F*). Thus, while the ON and OFF LS RGCs showed thresholds consistent with purely cone-driven responses (Deans *et al.* 2002), the HS, IS and LIS cells all responded within the rod-driven intensity range.

The present finding that ON and OFF RGCs in mouse retina could each be divided into largely distinct groups based on intensity–response profiles and threshold sensitivities is consistent with previous studies (Deans *et al.* 2002; Völgyi *et al.* 2004). However, those studies did not report ON cells within the LIS sensitivity range, although we consistently encountered them in our recordings. Our results thus indicate an overall symmetry in the intensity–response profiles and threshold sensitivities of ON and OFF RGC populations in the mouse retina, suggesting ON/OFF symmetry in the anatomy of the different rod pathways (Fig. 1). We also recorded from a very limited cohort of ON–OFF RGCs ($n = 35$) during the course of this study. These cells could be placed into each of the four categories based on the sensitivity of their ON or OFF responses, with most in the IS sensitivity range (HS = 3; IS = 21; LIS = 9; and LS = 2). However, because of their relatively low numbers we have not included them in subsequent phases of this study.

An interesting question is whether the different physiological groups based on threshold sensitivities consist

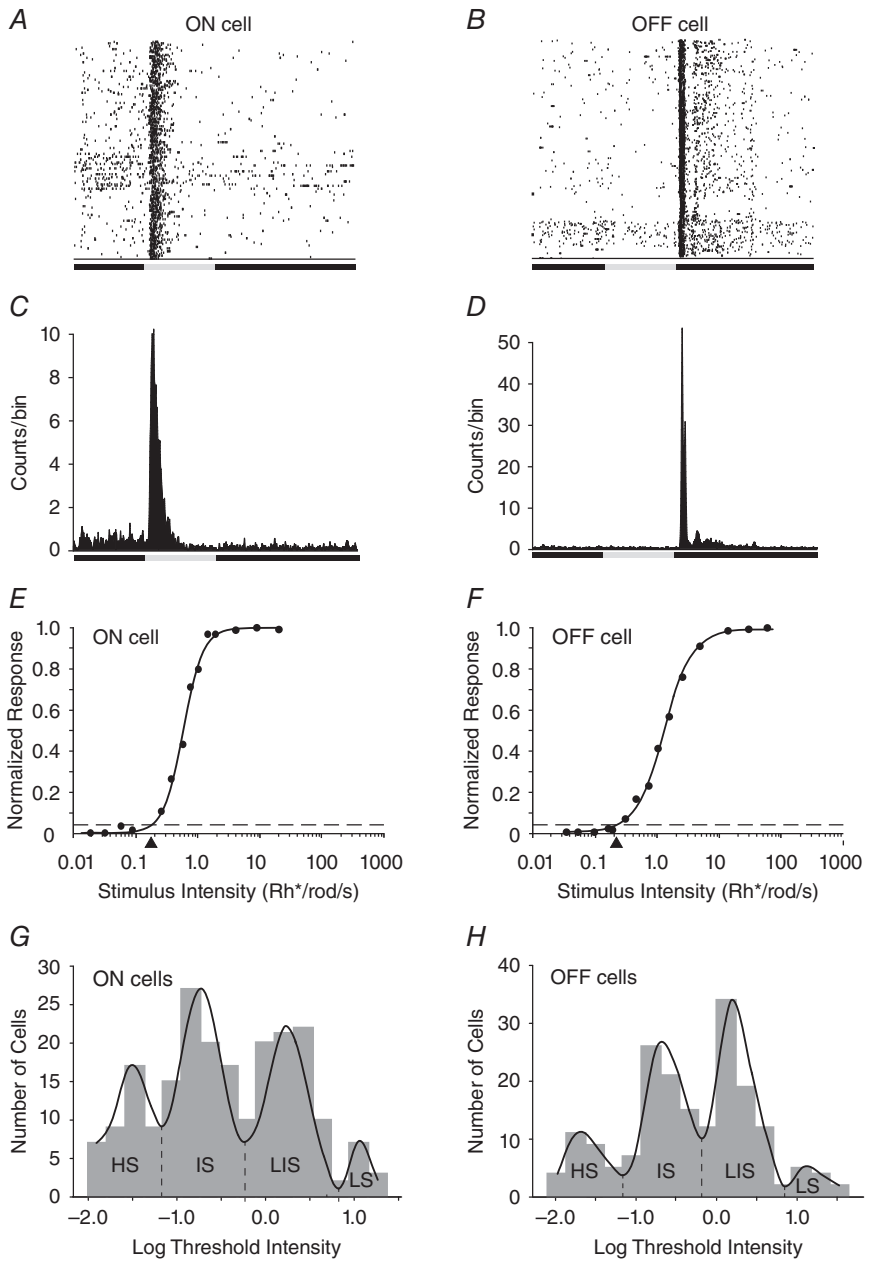


**Figure 2. Dark-adapted mouse retinal gangion cells (RGCs) are divisible by their different threshold sensitivities**
*A*, raster plot of multiple responses of an ON RGC to a 0.5 s full-field light stimulus. *B*, raster plot of multiple responses of an OFF cell to 0.5 s light stimulus. *C*, peristimulus time histogram of an ON RGC to 10 presentations of a 0.5 s full-field light stimulus. *D*, peristimulus time histogram of an OFF cell to a 0.5 s full-field light stimulus. *E*, intensity–response plot of an ON RGC with data points fitted by a Michaelis–Menten equation. The threshold sensitivity of the cell was calculated as 5% of the maximal response (spike frequency) and is indicated by the arrowhead below the *x*-axis and falls within the intermediate sensitivity range. *F*, intensity–response function of an OFF RGC with a threshold sensitivity (arrowhead) falling in the intermediate sensitivity range. *G*, histogram showing the range of threshold intensities calculated from the intensity–response functions of the population of dark-adapted ON RGCs in the study. Although the thresholds were found to be continuous, they could be differentiated into four groups [high (HS), intermediate (IS), low-intermediate (LIS) and low (LS) sensitivity], based on a non-linear regression fit. *H*, histogram showing the range of threshold intensities calculated from the intensity–response functions of the population of dark-adapted OFF RGCs in the study. Similar to that shown for the ON cells, the OFF cells could be differentiated into four groups [high (HS), intermediate (IS), low-intermediate (LIS) and low (LS) sensitivity], based on a non-linear regression fit of the threshold range.

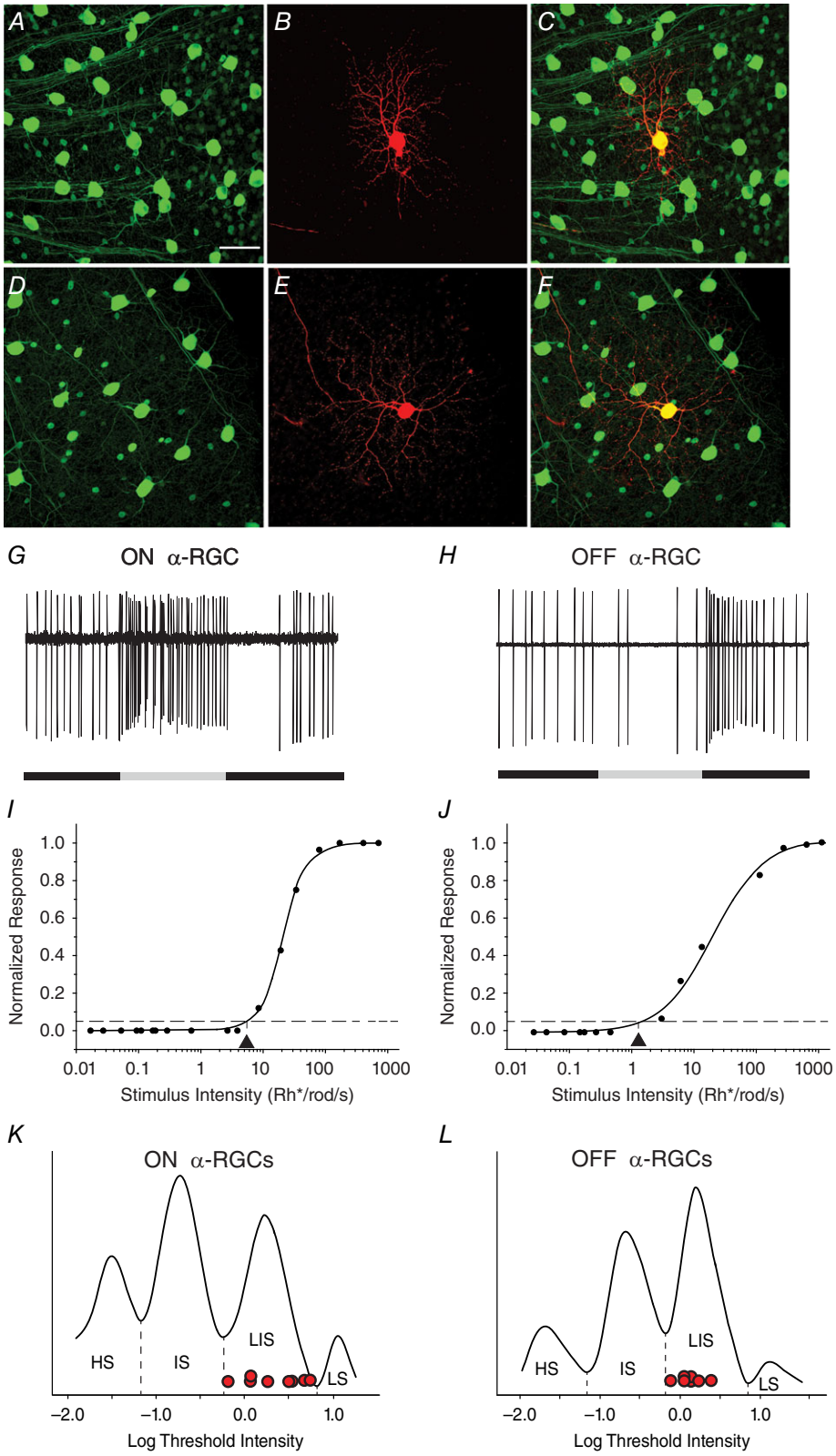


**Figure 3. Dark-adapted ON and OFF α-RGCs show threshold sensitivities consistently in the LIS range**
*A* and *D*, the α-RGCs in the Kcng4-YFP mouse retina express YFP and can be visualized and targeted for recording. Scale bar for panels *A*–*F* represents 50 μm. *B*, an ON α-RGC was targeted and injected with neurobiotin to reveal its soma–dendritic morphology. *C*, merge of *A* and *B*. *E*, an OFF α-RGC was targeted and injected with neurobiotin.

*F*, merge of *D* and *E*. *G*, spike response of the ON sustained $\alpha$-RGC shown in *A–C* to a 500 ms full-field light stimulation (intensity = 13.9 Rh* per rod $s^{-1}$). *H*, spike response of the OFF sustained $\alpha$-RGC shown in *D–F* to a 500 ms full-field light stimulation (intensity = 13.9 Rh* per rod $s^{-1}$). *I*, intensity–response function of the ON sustained $\alpha$-RGC, showing a threshold sensitivity of 0.65 Rh* per rod $s^{-1}$). *J*, intensity–response function of the OFF sustained $\alpha$-RGC, showing a threshold sensitivity of 1.5 Rh* per rod $s^{-1}$. *K* and *L*, distribution of threshold sensitivities of ON and OFF RGCs from Fig. 2*G* and *H*, respectively, with the threshold sensitivities of eight ON and eight OFF $\alpha$-RGCs (red circles) show that they all fall within the range of LIS cells. [Colour figure can be viewed at wileyonlinelibrary.com]

of different morphological subtypes of RGCs in the mouse retina. Although a definitive answer to this question would require a systematic study of the >20 RGC subtypes in the mouse retina (Sun *et al.* 2002; Badea & Nathans, 2004; Coombs *et al.* 2006; Völgyi *et al.* 2009), we focused on members of a single subtype to begin to address this issue. We determined the threshold sensitivity of ON and OFF sustained $\alpha$-RGCs, which express YFP in the Kcng4-YFP transgenic line (Duan *et al*, 2015) and can thereby be visualized and targeted for recording (Fig. 3*A–F*). We recorded the light-evoked activity of ON sustained ($n = 8$) and OFF sustained ($n = 8$) $\alpha$-RGCs to sequential presentations of different intensity stimuli and computed their threshold sensitivities from intensity–response profiles. We found that all the dark-adapted $\alpha$-RGCs showed thresholds within the LIS range of approximately 0.6–6.0 Rh* per rod $s^{-1}$ (Fig. 3*K* and *L*). Thus, the $\alpha$-RGCs fell within a single physiological group, consistently ~2 log units less sensitive than the most sensitive RGCs in the dark-adapted mouse retina.

## Blockade of GABAergic inhibition alters the threshold sensitivity of RGCs

Based on extracellular spike recordings, Völgyi *et al.* (2004) posited that the differences in the intensity–response profiles for the RGC groups was likely to be derived from an anatomical segregation of the three rod pathways with regard to their RGC targets. As available anatomical data argue against such a segregation (Raviola & Gilula, 1973; Cohen & Sterling, 1990*b*; Schneeweis & Schnapf, 1995; Tsukamoto *et al.* 2001; Veruki & Hartveit, 2002; Petrides & Trexler, 2008), we propose the following alternative hypothesis: RGCs receive convergent inputs from the three rod pathways, but signals carried by the pathways are masked differentially, resulting in the varied threshold sensitivities.

To test this idea, RGCs ($n = 195$) were first stimulated with light of increasing intensity in control conditions and then bathed in the non-selective GABA receptor blocker picrotoxin (PTX, 100 $\mu$M) for 15 min, after which the presentation of the sequential light stimuli was repeated (Fig. 4*A*). We first examined the effect of PTX on the sensitivity of LS ON and OFF RGCs, which showed only cone-driven responses in control conditions. Application of PTX most often produced an ~3 log unit increase in sensitivity, transforming ON and OFF LS RGCs cells into HS cells (Figs 4*B* and *C* and 5). However, we found that PTX could less often shift other LS cell thresholds to the sensitivity ranges typically seen for IS or LIS cells (Fig. 5). Approximately 10% of ON and OFF LS cells showed no change in their threshold sensitivity after PTX application. Overall, however, we found that PTX increased the sensitivity of ON and OFF LS ON cells by 1.80 ± 0.26 log units (mean ± SEM; $n = 19$).

We also found that application of PTX produced a leftward shift in the intensity–response functions of ON and OFF IS and LIS cells to thresholds most often within the threshold sensitivity range displayed by HS cells; average leftward shift of 1.23 ± 0.06 log units for ON and OFF IS cells ($n = 67$) and 1.03 ± 0.09 log units for ON and OFF LIS ON cells ($n = 69$; Figs 4*D* and 5). The latter cells included identified $\alpha$-RGCs, which showed an increase in sensitivity of 1.16 ± 0.12 log units ($n = 4$) after PTX application, similar to the change seen for other LIS RGCs. In contrast, we found that PTX never produced a significant change ($P > 0.1$) in the intensity–response functions of ON or OFF HS cells; average leftward shift of 0.04 ± 0.03 log units for ON and OFF ON HS cell ($n = 33$; Figs 4*E* and 5). Finally, we performed whole-cell voltage-clamp recordings to determine the effect of PTX application on the intensity–response properties of light-evoked EPSCs ($n = 7$). We observed that PTX brought about a leftward shift in the intensity–response function and threshold sensitivity of the EPSCs of individual RGCs in a manner comparable to that seen for their spike responses (Fig. 4*F* and *G*).

Overall, we found that application of PTX brought about an increase in sensitivity in 85% of the RGCs we examined. These changes were observed as a leftward shift of intensity–response curves of 1–3 log units, to ranges corresponding to the threshold sensitivities normally displayed by LIS, LS and, most often, HS cells. Our results are thus consistent with a tonic GABAergic inhibition, which reduces the threshold sensitivity of most RGCs by selectively masking rod signals derived from the different rod pathways. It should be noted that we found no statistically significant differences between sustained and transient RGCs within each of the four sensitivity categories for these and subsequent experiments. Therefore, data presented below

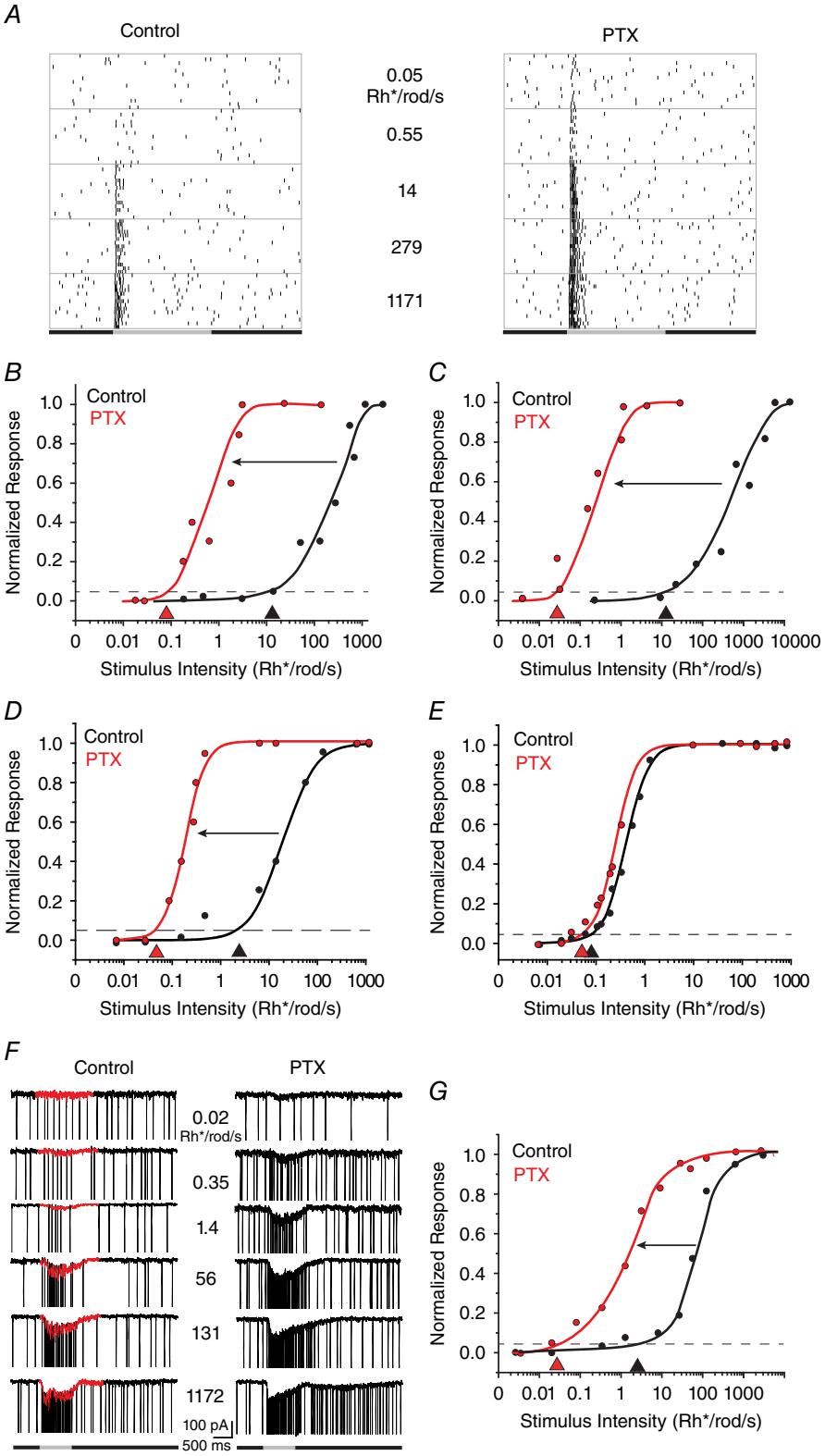


**Figure 4. Blockade of GABAergic inhibition increases threshold sensitivity of many RGCs**
*A*, raster plots of an ON RGC to a full-field light stimulus of increasing intensity in control conditions and after application of picrotoxin (PTX). Picrotoxin increased the threshold sensitivity of this LS ON cell from approximately 14 to 0.05 Rh* per rod $s^{-1}$. *B*, intensity–response profile of an LS ON RGC, showing an approximate 3 log unit

increase in threshold sensitivity after application of PTX. *C*, intensity–response profile of a LS OFF RGC showing an approximate 3 log unit increase in threshold sensitivity after application of PTX. *D*, intensity–response profile of an LS ON RGC showing an approximate 2 log unit increase in threshold sensitivity after application of PTX. *E*, intensity–response profile of an HS ON RGC showing that PTX did not increase the sensitivity of these cells. These results support the idea that HS responses are derived from the most sensitive primary rod pathway. *F*, amplitude of EPSCs of an ON LIS RGC to increasing full-field stimuli before and after the application of PTX. The fast, inward spike currents were removed graphically to isolate the EPSCs (red). *G*, intensity–response profiles of the data in *F*, showing that PTX increases the threshold sensitivity of the EPSC response by ∼2 log units. [Colour figure can be viewed at wileyonlinelibrary.com]

from sustained and transient RGCs have been grouped together within each of the four sensitivity categories.

### Light-evoked EPSCs and spike activity of individual RGCs show the same threshold sensitivity

In the next set of experiments, we determined whether the subthreshold ESPSs and spike responses of individual RGCs showed comparable intensity–response profiles and threshold sensitivities (Fig. 6*A*–*C*). We carried out this analysis on six RGCs, which, based on the light-evoked spike responses, were divided into different groups, including two LS ON cells, two LS OFF cells, one IS ON cell and an LIS OFF RGC. Figure 6*C* shows the intensity–response profiles for the EPSCs and spike responses of an OFF LIS RGC, which were very similar, with corresponding threshold sensitivities of 4.82 and 5.26 Rh* per rod $s^{-1}$, respectively. Overall, we found that the light-evoked EPSCs and spike responses of individual RGCs showed nearly identical intensity–response functions and calculated threshold sensitivities ($P > 0.1$, $n = 6$; Fig. 6*D*). Our results thus indicated that the most sensitive excitatory synaptic currents to RGCs were efficiently translated into a spike response.

### The inhibition affecting RGC sensitivity is subserved mainly by $GABA_C$ receptors

Picrotoxin has been shown to block glycine receptors in retinal neurons (Wang & Slaughter, 2005; Li & Slaughter, 2007), suggesting that at least part of the effects of PTX on RGC sensitivity could reflect blockade of glycinergic inhibition. In addition, glycinergic inputs from AII cells have been shown to contribute to the threshold of dark-adapted OFF RGCs (Müller *et al.* 1988; Arman & Sampath, 2012). To test for a potential glycinergic contribution to the PTX-induced changes in RGC sensitivity, we examined the effects of the glycine receptor antagonist strychnine (1 $\mu$M) on response threshold. Application of strychnine increased the spontaneous and light-evoked spike activity of most RGCs. However, consistent with previous studies (Müller *et al.* 1988; Arman and Sampath, 2012), we found that strychnine produced only a very small increase in the threshold of OFF RGCs (OFF HS, 0.17 ± 0.22 log units, $n = 3$; OFF IS, 0.19 ± 0.08 log units, $n = 3$) and a negligible increase ($P > 0.1$) of the threshold for ON RGCs (ON HS, 0.01 ± 0.01 log units, $n = 4$; ON IS, 0.01 ± 0.01, $n = 3$; Fig. 7*A*). These changes were far less than the 1–3 log unit changes in threshold produced by PTX, indicating that any contribution of glycinergic inhibitory pathways to these effects was insignificant. Thus, although strychnine clearly increased the excitability of RGCs, based on increased spontaneous and light-evoked spike activity, it had very minor effects on threshold sensitivity.

There are two major types of inhibition found in the inner retina: feedforward inhibition, in which ACs synapse directly onto RGCs, and feedback inhibition, where ACs synapse onto the axon terminals of BCs or dendrites of other ACs (Dowling & Boycott, 1966). In the rodent, $GABA_C$ receptors are found presynaptic to RGCs and thereby mediate feedback inhibition, whereas $GABA_A$ receptors are found on AC and RGC dendrites and BC axon terminals and can subserve both feedback and feedforward inhibition (Enz *et al.* 1996; Wässle *et al.* 1998; Lukasiewicz *et al.* 2004; Zhou & Dacheux, 2005; Sagdullaev *et al.* 2006; Eggers *et al.* 2007; Eggers & Lukasiewicz, 2010). Given that PTX blocks both $GABA_A$ and $GABA_C$ receptors, we used specific antagonists for these receptors to determine the role of each in modulating RGC sensitivity.

We found that application of the $GABA_A$ receptor blocker SR-95531 (SR, 10 $\mu$m) or the $GABA_C$ receptor blocker TPMPA (100 $\mu$m) had no significant effect ($P > 0.1$) on the sensitivity of ON or OFF HS cells (0.07 ± 0.06 log unit average change, $n = 37$), consistent with the actions of PTX (Fig. 6*B*). Likewise, SR had little effect on the intensity–response functions or threshold sensitivity of most ON and OFF IS RGCs (0.06 ± 0.06 log units, $n = 14$; Fig. 7*C*). Application of SR had almost no effect on the sensitivity of most ON or OFF LIS cells (0.11 ± 0.21 log unit average change, $n = 25$), but seven cells did show a 1–2 log unit shift in sensitivity. Application of SR also had little effect on the threshold sensitivity of most ON and OFF LS RGCs (0.10 ± 0.12 log unit average change, $n = 22$), although ∼20% of LS ON cells ($n = 7$) and 17% of LS OFF cells ($n = 6$) showed a 1–2 log unit increase in sensitivity (Fig. 7*D*–*F*). In contrast, exposing RGCs to TPMPA significantly increased the sensitivity of all ON and OFF IS RGCs (1.11 ± 0.44 log unit average change, $n = 20$), LIS cells (1.63 ± 0.19 log unit average

change, $n = 54$) and LS cells ($2.88 \pm 0.36$ log unit average change, $n = 12$; Fig. 7*C–F*).

## Direct feedforward inhibition to RGCs does not affect threshold sensitivity

The finding that $GABA_C$ receptors rather than $GABA_A$ receptors play a major role in controlling RGC threshold sensitivity suggests a mechanism involving feedback rather than direct feedforward inhibition. To test whether direct inhibition of RGCs was responsible for masking rod

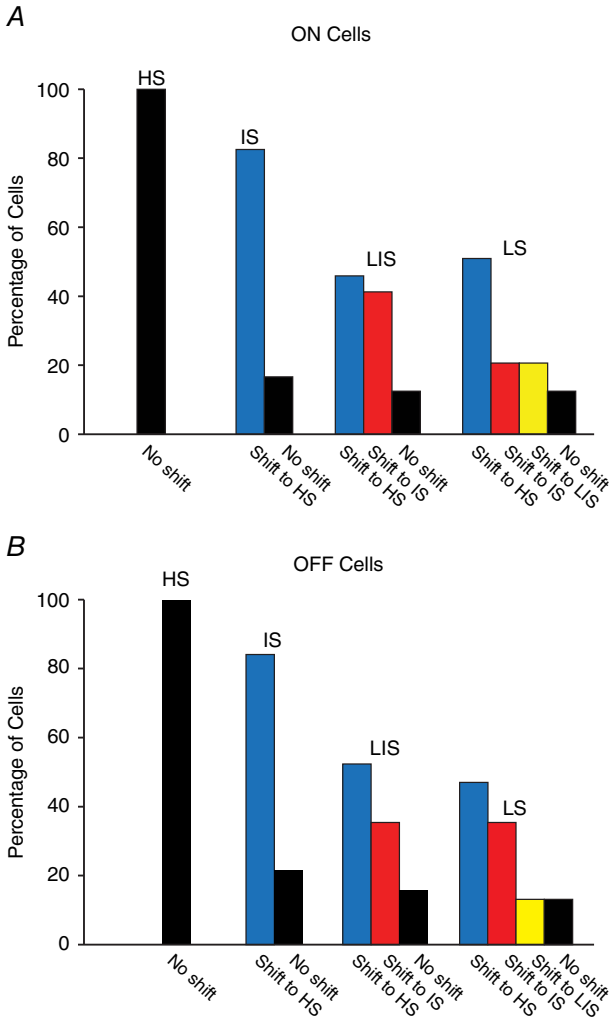


**Figure 5. Summary of the sensitivity changes induced by PTX as indicated by shifts in the intensity–response functions of individual cells**
*A*, application of PTX produced an increase of the threshold sensitivity of almost all IS, LIS and LS ON RGCs. Most shifts in sensitivity of IS and LS cells were to the range normally displayed by HS cells. However, PTX never increased the sensitivity of HS ON cells. *B*, application of PTX increased the sensitivity of most IS, LIS and LS OFF RGCs. However, as seen for ON cells, PTX did not alter the sensitivity of HS OFF RGCs. [Colour figure can be viewed at wileyonlinelibrary.com]

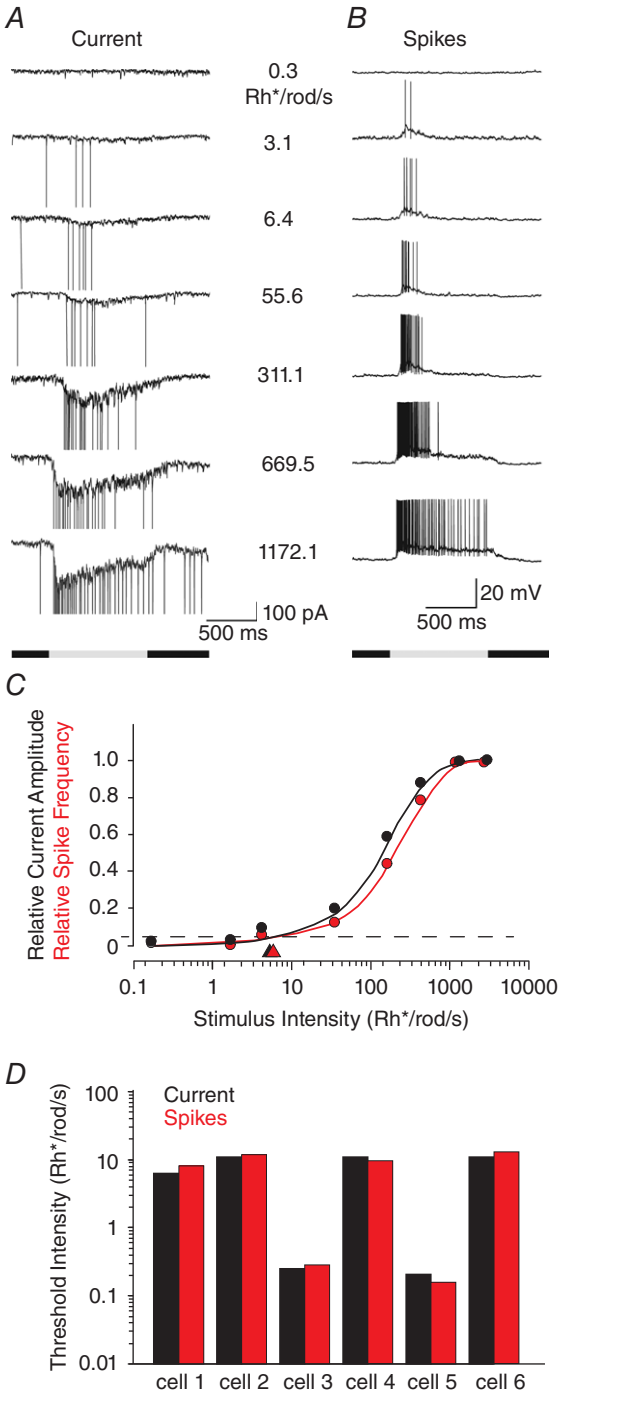


**Figure 6. The subthreshold and spike responses of single RGCs show similar threshold sensitivities**
*A*, EPSCs of an ON RGC evoked by full-field light of increasing intensity. *B*, spike responses of the same RGC as in *A* recorded in current-clamp mode to the same light stimuli. *C*, intensity–response functions computed for data shown in *A* and *B*. The threshold sensitivities (arrowheads) of the two functions are almost identical. *D*, histogram showing the threshold sensitivity of the subthreshold and spike responses recorded from six individual RGCs (two LS ON cells, two LS OFF cells, one IS ON cell and one LIS OFF cell). [Colour figure can be viewed at wileyonlinelibrary.com]

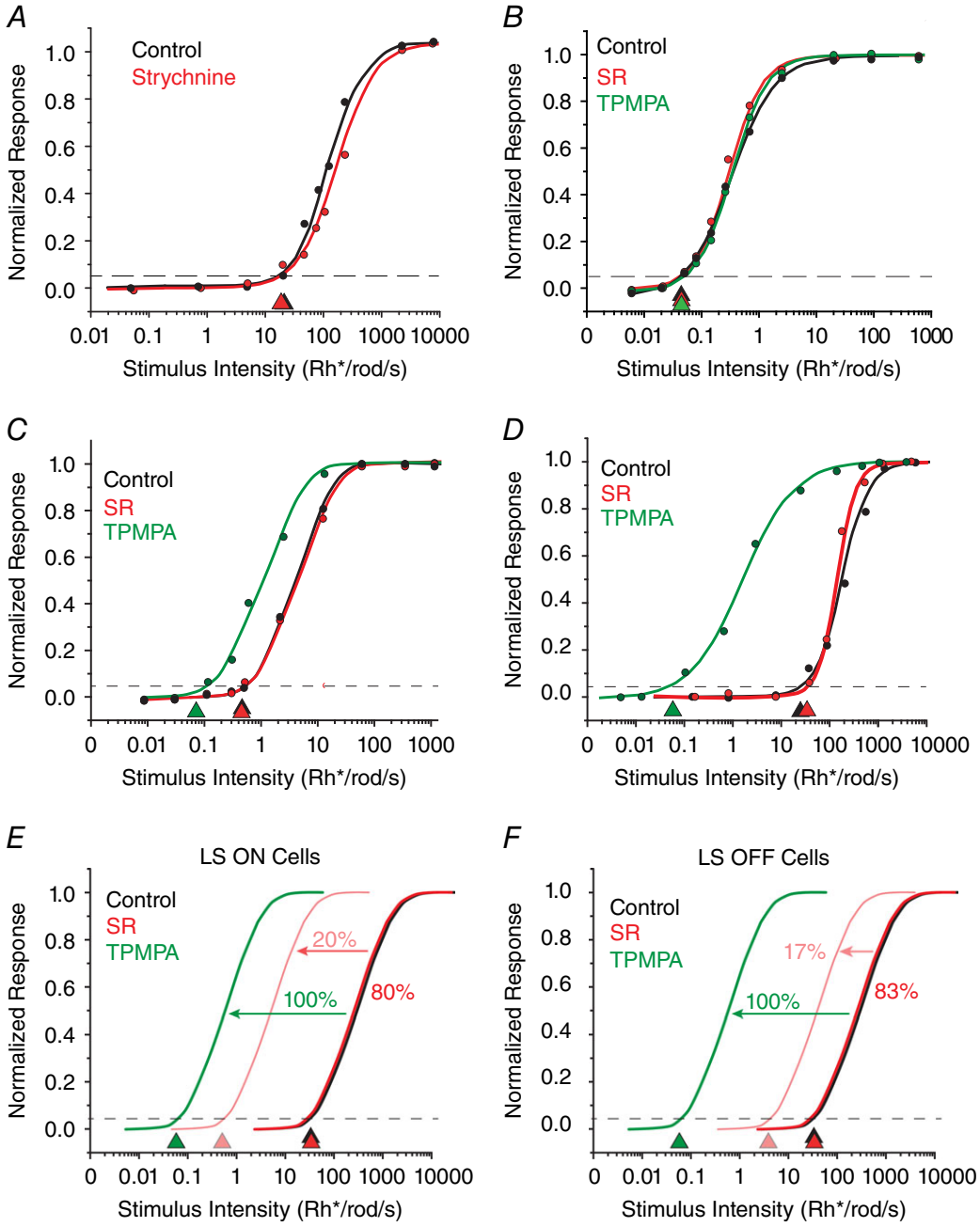


**Figure 7. Effects of selective GABA receptor blockers on RGC sensitivity**
*A*, application of the glycine receptor blocker strychnine had no significant effect on the intensity–response function and calculated threshold of an ON LS RGC. *B*, effects of the $GABA_A$-selective blocker gabazine (SR-95531) and the $GABA_C$-selective blocker 1,2,5,6-tetrahydropyridin-4-yl-methylphosphinic acid (TPMPA) on an ON HS RGC. Neither SR nor TPMPA had a significant effect on the threshold sensitivity of HS cells. *C*, data showing that SR had no effect on the sensitivity of an ON IS cell, but application of TPMPA increased the threshold sensitivity by ~1 log unit to the HS range. *D*, intensity–response functions for an OFF LS cell, showing that SR had no effect on the sensitivity of LS OFF cells, but TPMPA increased the sensitivity by ~3 log units. *E*, summary of the effects of SR and TPMPA on ON LS cells. Application of SR had no effect on the sensitivity of LS ON cells, but increased the sensitivity of 20% of LS ON cells, reflected by a leftward shift of intensity–response functions by 2 log units. In contrast, TPMPA increased the sensitivity of all LS ON cells by ~3 log units to the HS range. *F*, summary of effects of SR and TPMPA on OFF LS cells. Application of SR had no effect on the threshold sensitivity of 83% of LS OFF cells, but increased the sensitivity of 17% of LS OFF cells, reflected by a leftward shift of intensity–response curves by an average of only ~1 log unit. In contrast, TPMPA increased the sensitivity of all LS OFF cells by ~3 log units to the HS range. [Colour figure can be viewed at wileyonlinelibrary.com]

signals, we performed whole-cell patch recordings of RGCs and held the membrane potentials at −60 and 0 mV, to isolate inward excitatory currents from outward inhibitory currents, respectively. At a holding potential of −60 mV, application of TPMPA produced a robust increase in the light-evoked excitatory, inward current (increase of 56.6 ± 17.4%; $n = 9$; Fig. 8*A*). However, this was coupled with only a small decrease (9.9 ± 10.5%) in the inhibitory, outward current, consistent with the blockade of inhibition presynaptic to the recorded RGCs. Application of TPMPA also resulted in a nearly 2 log unit increase in threshold sensitivity for the cell data in

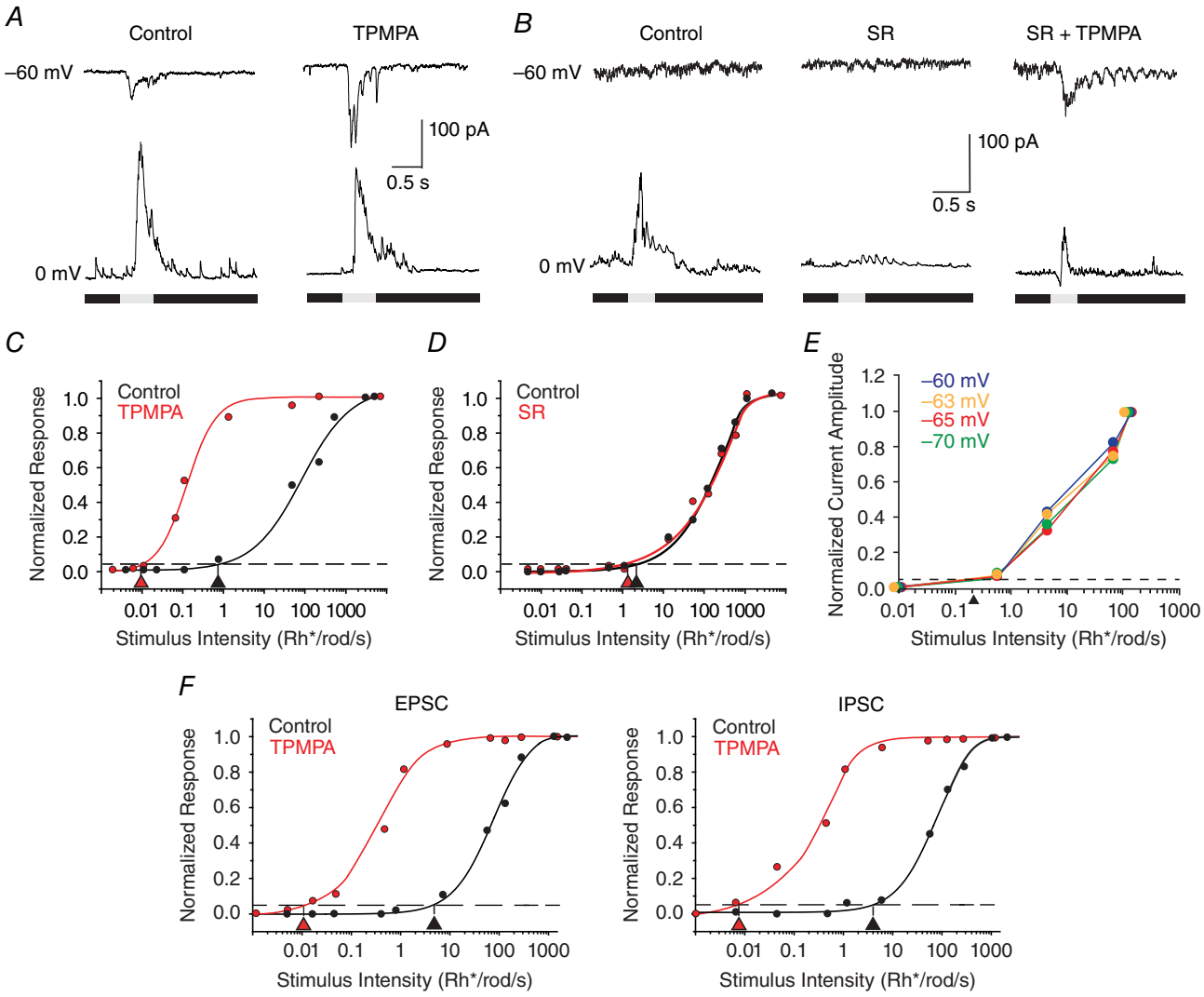


**Figure 8. Voltage-clamp recordings indicate that inhibition that affects threshold sensitivity is not directly on RGCs**
*A*, light-evoked current of an RGC voltage clamped at −60 and 0 mV to isolate excitatory and inhibitory currents, respectively. Application of TPMPA revealed a large excitatory, inward current, but had little effect on the inhibitory outward current evoked in control conditions. The stimulus intensity was 6.4 Rh* per rod $s^{-1}$. *B*, application of SR blocked the direct inhibitory current evoked by light, but did not reveal an excitatory current. However, application of SR and TPMPA did reveal an excitatory inward current, although this was coupled with a small outward current. The stimulus intensity was 0.1 Rh* per rod $s^{-1}$, below threshold sensitivity in control conditions. *C*, application of TPMPA produced an ∼2 log unit increase in sensitivity of the recorded EPSCs recorded from the same RGC as shown in *A*. *D*, application of SR had no effect on the threshold sensitivity of the EPSCs recorded from same cell as shown in *B*. *E*, EPSCs recorded from an OFF IS RGC in response to different intensity light stimuli at holding potentials of −60, −63, −65 and −70 mV. Normalized intensity–response functions indicate no significant change in the threshold as calculated from the EPSCs evoked at the different holding potentials. *F*, intensity–response functions for the EPSCs and IPSCs recorded in an ON LIS RGC in response to different stimulus intensities. The EPSCs and IPSCs showed similar threshold sensitivity values in control conditions and a similar increase in sensitivity after application of TPMPA. [Colour figure can be viewed at wileyonlinelibrary.com]

Fig. 8*C* (ON and OFF HS cells, $n = 3$, $0.16 \pm 0.05$ log unit change; ON and OFF IS cells, $n = 5$, $1.65 \pm 0.59$ log unit change; ON and OFF LIS cells, $n = 6$, $1.86 \pm 0.33$ log unit change; ON and OFF LS cells, $n = 3$, $1.99 \pm 0.71$ log unit change). In contrast, application of the $GABA_A$ blocker SR did produce a significant decrease ($74.7 \pm 9.0\%$) in the direct, light-evoked inhibition of RGCs, but surprisingly, this did not translate into a large increase in the excitatory inward current (increase of $11.6 \pm 11.8\%$, $n = 11$, $P > 0.1$; Fig. 8*B*). As a result, the threshold sensitivity of RGCs, as assayed by synaptic current recordings, was not significantly influenced by application of SR (ON and OFF HS cells, $n = 6$, $0.06 \pm 0.05$ log unit change; ON and OFF IS cells, $n = 6$, $0.20 \pm 0.08$ log unit change; ON and LIS cells, $n = 7$, $0.12 \pm 0.26$ log unit change; ON and OFF LS cells, $n = 3$, $0.14 \pm 0.16$ log unit change, $P > 0.1$ for all comparisons), consistent with the results based on spike analyses (Fig. 8*D*). Interestingly, subsequent application of TPMPA (SR+ TPMPA) did produce a large increase ($399.0 \pm 89.6\%$) in the outward inhibitory current compared with control levels, which was coupled with an increase in the excitatory, light-evoked inward currents compared with SR levels, but a decrease from control levels ($-28.1 \pm 16.3\%$; Fig. 8*B*), similar to the effects of applying of TPMPA alone. Application of TMPA + SR, as for PTX, resulted in a large increase in threshold sensitivity (ON and OFF IS cells, $n = 3$, $1.62 \pm 0.20$ log unit change; ON and OFF LIS cells, $n = 4$, $1.83 \pm 0.52$ log unit change). Thus, the amount of direct inhibition of RGCs did not correlate with the level of excitation or the change in threshold sensitivity produced by the addition of selective GABA receptor blockers.

In the next series of experiments, we voltage clamped RGCs near $E_{Cl}$ to determine whether suppression of direct chloride inhibition could influence threshold sensitivity. Owing to the probability of an imperfect space clamp of large, spontaneously active RGCs, these cells were voltage clamped to a number of potentials ranging from $-60$ to $-70$ mV. The EPSC amplitudes were then measured at these different holding potentials in response to a range of stimulus intensities (Fig. 8*E*). Normalized intensity–response functions were then computed at each holding potential to determine whether there was a change in threshold. Although the EPSCs elicited by a given stimulus varied in amplitude with the different holding potentials, the thresholds calculated from the normalized intensity–response curves showed no changes ($0.05 \pm 0.03$, $n = 5$; constant threshold of $\sim$0.2 Rh* per rod $s^{-1}$ for the RGC responses illustrated in Fig. 8*B*). Thus, suppression of direct inhibition to RGCs did not alter their threshold sensitivity.

We also compared the threshold sensitivities of the EPSCs and IPSCs recorded in individual LS ($n = 6$) and LIS RGCs ($n = 4$) in control conditions and after TPMPA application. We found that the EPSCs and IPSCs in individual LS cells showed similar sensitivities in control conditions (log $2.52 \pm 0.16$ and $2.48 \pm 0.01$, respectively) and both shifted to a higher sensitivity of $\sim$3 log units (log $0.14 \pm 0.11$ and $0.13 \pm 0.01$, respectively) after TPMPA was applied. Likewise, the EPSCs and IPSCs of LIS cells showed similar threshold sensitivities (log $1.31 \pm 0.09$ and log $1.42 \pm 0.06$, respectively) and both shifted $\sim$2 log units more sensitive after TPMPA application (log $-1.09 \pm 0.04$ and log $-1.08 \pm 0.06$, respectively; Fig. 8*F*). Thus, the postsynaptic inhibition in these cells did not show a higher sensitivity necessary to mask signals from the primary and secondary rod pathways. Furthermore, the increased sensitivity of IPSCs seen after TPMPA application was opposite to that change expected if this postsynaptic inhibition was responsible for masking the higher sensitivity signals. Taken together, these data provide further evidence in support of a presynaptic mechanism for the masking inhibition.

## Blockade of GABAergic inhibition produces minimal changes in the sensitivity of RGCs in the Cx36$^{-/-}$ mouse retina

We next examined the effects of PTX on the response sensitivity of RGCs in the Cx36$^{-/-}$ mouse retina. It has been previously shown that deletion of Cx36-expressing gap junctions has profound effects on signalling via the rod pathways, including a complete loss of signalling via the secondary rod pathway, a loss of ON signalling via the primary rod pathway and an $\sim$1 log unit loss of sensitivity of OFF signals carried by the primary rod pathway (Deans *et al.* 2002; Völgyi *et al.* 2004). Therefore, if the shifts in sensitivity produced by application of PTX described above were the result of an unmasking of inputs from the different rod pathways, then PTX effects on RGCs in the Cx36$^{-/-}$ mouse retina, in which not all rod pathways are operational, should necessarily be different from that produced in WT retinas.

Consistent with previous findings, we found that ON and OFF HS RGCs and ON IS RGCs were absent in the Cx36$^{-/-}$ mouse retina, presumably because of functional loss of the primary and secondary rod pathways (Deans *et al.* 2002; Völgyi *et al*, 2004). Moreover, we found that application of PTX produced no significant change in the sensitivity of ON LIS RGCs ($0.07 \pm 0.10$ log units, $n = 12$) and most ON LS RGCs ($0.31 \pm 0.13$ log units, $n = 10$), in clear contrast to the effects seen in WT retinas (Fig. 9*A* and *B*). These results can be explained by the loss of the primary and secondary rod pathways in the Cx36$^{-/-}$ mouse retina whereby there were no higher sensitivity signals to be unmasked by PTX. In contrast, application of PTX did produce a significant increase in sensitivity of OFF LS ($1.97 \pm 0.38$ log units, $n = 5$) and OFF LIS

RGCs (0.91 ± 0.15, $n = 10$; Fig. 9*C* and *D*). It should be noted that the leftward shift of the intensity–response functions of these OFF cells was most often to the HS range (indicated by an asterisk in Fig. 9*D*), which was shifted ∼1 log unit to the left, occupying the range normally occupied by the IS cells. This is because the HS RGCs are ∼1 log unit less sensitive in the Cx36$^{-/-}$ mouse retina than in the WT, reflecting an ∼1 log unit loss in sensitivity of OFF signals carried by the primary rod pathway because of uncoupling of AII ACs (Völgyi *et al.* 2004). Consistent with results in WT retinas, application of PTX did not alter the threshold sensitivity of presumed OFF HS cells. Overall, our results from the Cx36$^{-/-}$ mouse support the idea that the GABAergic inhibition masks scotopic signals with different sensitivities, which are carried discretely by the three rod pathways.

## The effects of GABAergic inhibition on RGC sensitivity are independent of dopaminergic circuitry

It has been shown that activation of dopaminergic circuits can influence the sensitivity of neurons in both the inner and outer retina (Li & Dowling, 2000; Herrmann *et al.* 2011). It was thus possible that the increased sensitivity of RGCs following GABA receptor blockade could involve an increase in dopamine release, owing to removal of a presumed tonic inhibition and the subsequent activation of dopaminergic circuits. To test this idea, we investigated whether the effects of GABA receptor blockage on RGC response sensitivity could be reversed by blockade of dopamine receptors.

In initial experiments, we found that application of the selective $D_2$ receptor blocker eticlopride (25 $\mu$M)

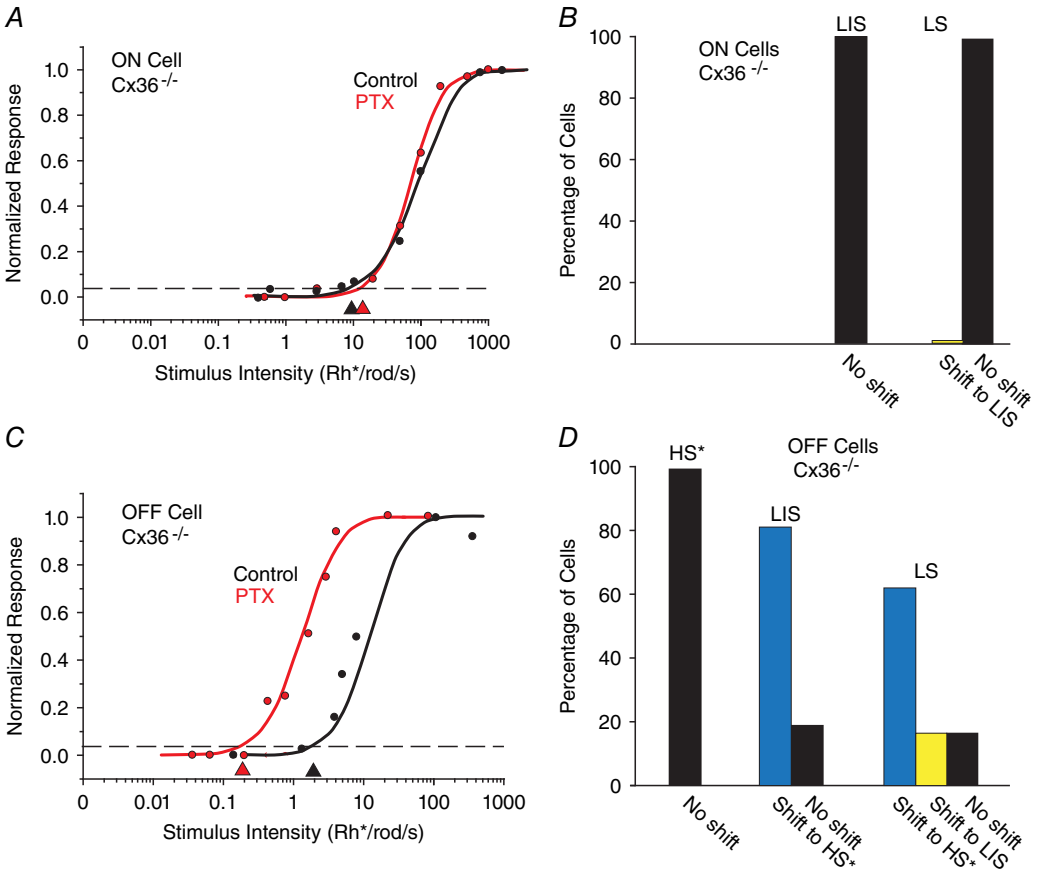


**Figure 9. Ablation of certain rod pathways in the Cx36$^{-/-}$ mouse retina indicates that the three pathways carry rod signals with different sensitivities**
*A*, the intensity–response function of an LS ON RGC in the Cx36$^{-/-}$ mouse retina is unaffected by application of PTX. This is likely to be attributable to the fact that the primary and secondary rod pathways are dysfunctional in the Cx36$^{-/-}$ mouse. *B*, histogram showing that PTX did not increase the sensitivity of ON LS cells in the Cx36$^{-/-}$ mouse retina, a clear contrast from the increased sensitivity seen in the wild-type (WT). *C*, application of PTX shifted the sensitivity of an OFF LS cell by ∼1 log unit to the LIS range. *D*, summary of the effects of PTX on OFF RGCs in the Cx36$^{-/-}$ mouse retina. Most cells showed a shift in sensitivity to the range of presumed HS cells (*) that show reduced sensitivity in the Cx36$^{-/-}$ mouse. Although PTX increased the sensitivity of most LIS and LS cells, it did not change the sensitivity of presumed HS cells (*) in the knockout. [Colour figure can be viewed at wileyonlinelibrary.com]

reduced the threshold sensitivity of all RGC types as follows: ON and OFF HS cells ($n$ = 32) reduced by 0.39 ± 0.10 log units; ON and OFF IS cells ($n$ = 56) reduced by 0.31 ± 0.41 log units; ON and OFF LIS cells ($n$ = 7) reduced by 0.22 ± 0.26 log units; and ON and OFF LS cells ($n$ = 2) reduced by 0.30 ± 0.52 log units (Fig. 10*A*). However, subsequent application of PTX with maintained $D_2$ receptor blockade increased the sensitivity of ON and OFF IS, LIS and LS cells beyond control levels to threshold values seen after PTX application alone (Fig. 10*A*; IS cells, 1.29 ± 0.53 log units from control levels, $n$ = 56; LIS cells, 1.15 ± 0.27 log units, $n$ = 7; LS cells, 1.81 ± 0.77 log units, $n$ = 2).

In a second set of experiments, we applied PTX first followed by the $D_2$ receptor blocker eticlopride. Consistent with our earlier findings, application of PTX had almost no effect on the sensitivity of ON and OFF HS cells (0.04 ± 0.02 log unit change, $n$ = 7, $P$ > 0.1). As shown in earlier experiments, PTX increased the threshold sensitivities of ON and OFF IS, LIS and LS cells (IS cells, 1.32 ± 0.72 log units, $n$ = 7; LIS cells, 1.02 ± 0.16 log units, $n$ = 24; LS cells, 1.45 ± 0.55 log units, $n$ = 2).

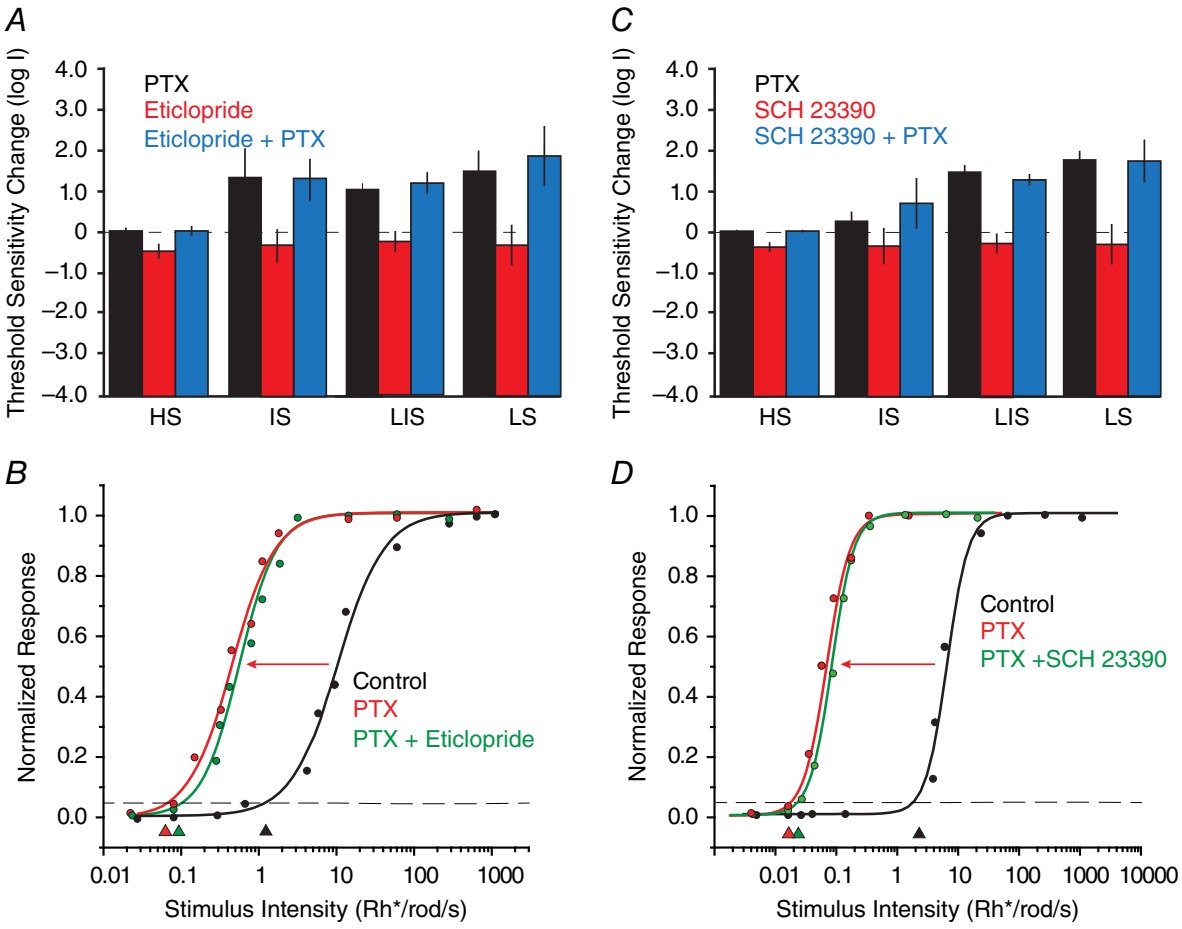


**Figure 10. Effects of blocking dopaminergic circuitry on RGC sensitivity**
*A*, histogram summarizing the effects of the $D_2$ receptor blocker eticlopride (25 $\mu$M) and PTX (100 $\mu$M) on the threshold sensitivity of the four classes of RGCs. With the exception of HS cells, PTX increased the threshold sensitivity of RGCs. In contrast, application of eticlopride reduced the sensitivity of RGCs. After eticlopride application, PTX still increased the sensitivity of RGCs to levels similar to those seen with PTX alone. *B*, example of an OFF LIS cell for which application PTX resulted in an ∼2 log unit increase in sensitivity, indicated by the leftward shift of the intensity–response function. However, subsequent application of eticlopride did not significantly reverse the PTX effect. Arrowheads indicate threshold sensitivity measured as 5% of maximal response. *C*, histogram summarizing the effects of the $D_1$ receptor blocker SCH 23390 (10 $\mu$M) and PTX on the threshold sensitivity of the four classes of RGCs. Picrotoxin increased the sensitivity of most RGCs, whereas SCH 23390 reduced the sensitivity. After application of SCH 23390, superfusion with PTX increased the sensitivity of RGCs to levels similar to those seen with PTX alone. However, after application of PTX, superfusion of SCH 23390 did significantly reverse the increase in GC threshold. *D*, example of an OFF LIS cell for which application PTX resulted in an ∼2 log unit increase in sensitivity indicated by the leftward shift of the intensity–response function. However, subsequent application of SCH 23390 did not significantly reverse the PTX effect. [Colour figure can be viewed at wileyonlinelibrary.com]

Subsequent application of eticlopride in the presence of PTX had no significant effect of the response sensitivity of ON and OFF HS, IS, LIS and LS cells (HS cells, 0.06 ± 0.03 log units from PTX-derived levels, $n = 6$; IS cells, 0.09 ± 0.08, $n = 23$; LIS cells, 0.13 ± 0.08 log units, $n = 24$; LS cells, 0.03 ± 0.01, $n = 2$). Thus, blockade of $D_2$ receptors had no significant effect on the increased sensitivity of RGCs produced by PTX application (Fig. 10*B*).

In the next phase of experiments, we examined the effects of blockade of $D_1$ receptors on the effects of PTX on RGC response sensitivity. Application of the $D_1$ receptor blocker SCH 23390 (10 $\mu$M) resulted in a decreased sensitivity of ON and OFF HS, LS, LIS and LS RGCs (HS cells, 0.78 ± 0.23 log units, $n = 7$; IS cells, 0.45 ± 0.11 log units, $n = 26$; LIS cells, 0.59 ± 0.20 log units, $n = 15$; LS cells, 0.81 ± 0.92, $n = 3$; Fig. 10*C*). Subsequent application of PTX in the presence of SCH 22390 increased the sensitivity of ON and OFF HS, IS, LIS and LS cells to threshold values similar to those found after PTX application alone (HS cells, 0.02 ± 0.01 log unit change from control values, $n = 7$; IS cells, 0.72 ± 0.66 log unit change, $n = 26$; LIS cells, 1.20 ± 0.16 log unit change, $n = 8$; LS cells, 1.72 ± 0.55 log unit change, $n = 3$; Fig. 10*C*). Thus, application of PTX reversed the sensitivity loss produced by $D_1$ receptor blockade and increased the threshold sensitivity to values seen with PTX application alone (Fig. 10*C*).

Finally, we examined whether blockade of $D_1$ receptors could reverse the increased sensitivity of RGCs produced by application of PTX. Consistent with aforementioned results, PTX had no effect ($P > 0.1$) on the sensitivity of ON and OFF HS cells (0.01 ± 0.01 log units, $n = 2$) but increased the sensitivity of ON and OFF IS cells (1.25 ± 0.22 log units, $n = 9$), LIS cells (1.44 ± 0.18 log units, $n = 18$), and LS cells (1.78 ± 0.2 log units, $n = 3$). Subsequent application of SCH 22390 in the presence of PTX produced no significant decrease in the sensitivity of ON and OFF HS cells (0.02 ± 0.01 log units, $n = 3$), IS cells (0.16 ± 0.23 log units, $n = 9$), LIS cells (0.21 ± 0.21 log units, $n = 12$) or LS OFF cells (0.17 ± 0.18 log units, $n = 3$; Fig. 10*D*). Overall, these data indicate that the increased sensitivity changes produced by PTX could not be reversed by blockade of dopamine actions through $D_1$ receptors.

## Discussion

We found that RGCs maintained in the same dark-adapted conditions showed a wide range of threshold sensitivities covering >3 log units, confirming earlier findings (Balkema & Pinto, 1982; Stone & Pinto, 1993; Lee *et al.* 1997; Deans *et al.* 2002; Völgyi *et al.* 2004). Although the thresholds of individual ON and OFF cells formed a continuum, they could still be segregated into four groups based on their peak distribution. Following the classification scheme used previously (Deans *et al.* 2002; Völgyi *et al.* 2004), the LS cells showed responses above cone thresholds, indicating a lack of rod-driven responses, whereas the HS, IS and LIS cells all responded mainly within the scotopic range. These results are consistent with a symmetrical organization whereby the primary rod pathway carries the most sensitive rod signals, whereas the secondary and tertiary pathway propagate scotopic signals that are 1–2 log units less sensitive (Sharpe & Stockman, 1999; Tsukamoto *et al.* 2001; Field & Rieke, 2002; Sampath & Rieke, 2004; Völgyi *et al.* 2004). In contrast to earlier studies, we found a substantial number of ON LIS RGCs in addition to the previously reported OFF LIS cells. This difference is likely to reflect the fact that the present study included a significantly larger database of RGCs than in previous studies. This new finding indicates symmetry in the third rod pathway, in which rods make chemical synapses with classes of both ON and OFF BCs (Blakemore & Rushton, 1965*a*,*b*; Fyk-Kolodziej *et al.* 2003; Li *et al.* 2004; Tsukamoto *et al.* 2007; Pang *et al.* 2010).

Our finding that ON and OFF $\alpha$-RGCs in dark-adapted retinas consistently maintained threshold sensitivities placing them in the LIS category supports the idea that the different physiological categories are composed of different morphological subtypes of RGCs. Clearly, $\alpha$-RGCs did not respond to the dimmest stimuli, indicating that they do not play a role in encoding the most sensitive visual responses, consistent with the findings of Pang *et al.* (2003). Interestingly, these results suggest that different cohorts of RGCs will be active over the scotopic intensity range. The strategy behind such an organization is unclear and even counterintuitive, in that not all RGCs would contribute to retinal signalling at a given dim ambient light level. One possibility is that this mechanism serves to limit the signals carried centrally via the optic nerve, whose limited bandwidth forms a bottleneck in the visual pathways, possibly increasing efficiency of dim-light signalling when spatial acuity takes a back seat to sensitivity. Clearly, study of the >20 other subtypes of RGCs is called for to determine their individual contribution to rod signalling.

The major focus of this study was to address the unresolved question of whether the multiple rod pathways converge onto single RGCs or innervate different subtypes. DeVries & Baylor (1995) reported that the primary and secondary pathways are mostly segregated in the rabbit retina, selectively targeting brisk or sluggish cells, whereas the two pathways were reported to converge onto single RGCs in the mouse retina (Soucy *et al.* 1998). Our initial finding that dark-adapted RGCs have a broad range of threshold sensitivities would seem to support segregated signalling of the rod pathways. However, the selectivity in

rod–cone and AII AC–ON cone BC coupling necessary to support such a segregation does not exist, at least in the mouse (Raviola & Gilula, 1973; Cohen & Sterling, 1990*a*; Schneeweis & Schnapf, 1995; Tsukamoto *et al.* 2001; Veruki & Hartveit, 2002; Petrides & Trexler, 2008). The present finding that manipulation of GABAergic inhibition alters the threshold sensitivity of RGCs supports an alternative explanation for the apparent segregation of the rod pathways. In this scheme, there is a convergence of the rod pathways onto individual RGCs, but inhibitory circuits subserved by ACs selectively mask inputs so that the rod signalling from a particular pathway will predominate. Four lines of evidence indicate that the site of the masking inhibition is mainly presynaptic to the RGCs. First, we found that blockade of $GABA_C$ receptors, which are expressed exclusively on BC axon terminals in the rodent retina (Enz *et al.* 1996; Wässle *et al.* 1998; Eggers *et al.* 2007; Eggers & Lukasiewicz, 2010), increased the threshold sensitivity in almost all RGCs, whereas blockade of $GABA_A$ receptors affected the sensitivity of only a few cells. Second, although most RGCs clearly receive direct inhibitory input from ACs (Field & Rieke, 2002; Sampath & Rieke, 2004), we found that the thresholds of the EPSCs matched those of the spike responses of individual cells. This finding argues that direct inhibition did not prevent synaptic signals from being expressed as a spike code, which would manifest as a reduction in the computed threshold sensitivity. Third, we found that amplitude or sensitivity changes in the direct inhibition of RGCs, measured as outward currents, did not correlate with changes in threshold sensitivity. For LS cells, the EPSCs and IPSCs showed similar threshold sensitivities both in control conditions and after TPMPA application, which would not be expected if the masking inhibition was directly on RGCs. Fourth, holding RGCs at $E_{Cl}$ and thereby eliminating direct inhibition did not alter their threshold sensitivities. If direct inhibition was in fact controlling the inhibition, then an increase in sensitivity should have resulted when chloride-mediated inhibition was negated. The feedback nature of the masking inhibition suggests that its modulation would probably not affect threshold sensitivity on a cell-by-cell basis, but rather would alter that of entire subtypes of RGCs postsynaptic to the same cohort of BCs, consistent with our findings for $\alpha$-RGCs. This organization would allow for selective control of the sensitivity of different RGC subtypes by altering the excitatory–inhibitory balance of their synaptic drive.

An important consideration is whether the pharmacological blockade of GABA receptors produced a generalized increase in RGC excitability and not the unmasking of signals derived from the different rod pathways. Several findings argue strongly against this. First, we found that there was generally no clear relationship between the effect of a drug on RGC inhibition–excitation and threshold sensitivity. Application of TPMPA reduced the inhibition to RGCs only slightly, yet it produced a significant increase in excitation and enhanced sensitivity. In contrast, application of SR significantly reduced direct RGC inhibition, yet there was no clear increase in excitation or sensitivity. Application of strychnine produced the greatest increase in RGC excitability yet had little effect on threshold sensitivity, while the dopaminergic blockers had opposing effects on excitability and sensitivity. Second, application of GABA blockers never produced an increase in the sensitivity of HS cells, consistent with the idea that they already carried the most sensitive rod signals derived from the primary rod pathway. Third, we found that cells did not show a sensitivity shift to a level corresponding to the signals carried by a particular rod pathway after it was deactivated in the $Cx36^{-/-}$ mouse retina. For example, in contrast to findings in WT mice, ON LIS cells did not show an increase in threshold sensitivity following GABA blockade in the $Cx36^{-/-}$ mouse, in which both the primary and secondary rod pathways were non-functional. Our results thus indicate that the effect of GABA blockade on threshold sensitivity was not an epiphenomenon of an overall increase in cell excitability. Rather, the present data are consistent with a tonic feedback inhibition that selectively masks rod signals derived from the different rod pathways, thereby controlling RGC sensitivity. It is therefore important to stress that direct cell excitability, as determined from spiking and current levels, was, with the exception of TPMPA, not correlated with the threshold sensitivity as computed from intensity–response functions. Taken together, these findings strongly support the idea that synaptic interactions presynaptic to RGCs are mainly responsible for controlling their sensitivities in scotopic conditions.

We posit that the masking inhibition occurs on bipolar cell axon terminals subserved mainly by $GABA_C$ receptors. Furthermore, this inhibition is likely to be limited to cone bipolar cells, which are elements within the primary, secondary and tertiary rod pathways (Fig. 1). Feedback inhibition directly onto rod bipolar cell axon terminals would result in an attenuation or loss of all high-sensitivity signals carried by the primary rod pathway to all RGCs and ACs. A scenario more parsimonious with our results is that the masking inhibition occurs on the more numerous cone bipolar cells, thereby providing the diversity in circuitry necessary to alter the threshold sensitivities of different cohorts of RGCs.

With >30 different morphological subtypes of amacrine cells in the retina (Masland, 2012), it remains unclear which of these subserve the feedback inhibition that controls threshold sensitivity of the RGCs. In addition, it is uncertain whether these same circuits are responsible

for others types of inhibition found in the inner retina, such as surround or lateral inhibition. There is strong evidence from a number of species that RGC surrounds are minimized or abolished in the dark-adapted conditions we used in the present study (Rodieck & Stone, 1965; Maffei *et al.* 1971; Cleland *et al.* 1973; Peichl & Wässle, 1983; Muller & Dacheux, 1997; Farrow *et al.* 2013). However, in the mouse retina, Farrow *et al.* (2013) reported that while large-field RGCs showed attenuated antagonistic surround receptive fields in scotopic conditions, the surrounds of some small-field RGCs remained. Given that we used full-field light stimulation in the present study, it is possible that the GABAergic inhibition controlling the threshold sensitivity of certain RGC subtypes was surround mediated. However, we found that large-field $\alpha$-RGCs showed threshold sensitivities in the LIS range, which could be shifted to higher sensitivity levels by application of PTX. As $\alpha$-RGCs lack surround receptive fields in scotopic conditions (Farrow *et al.* 2013), these data suggest that, at least for this subtype of RGC, the feedback circuitry responsible for the inhibition that controls threshold sensitivity must be distinct from that which mediates surround inhibition.

Previous work has shown that activation of dopaminergic circuits can increase the sensitivities of neurons throughout the retina (Li & Dowling, 2000; Herrmann *et al.* 2011). Our results confirmed that obstructing these circuits by blocking $D_1$ or $D_2$ receptors reduced the threshold sensitivities of most RGCs in the mouse retina. However, blockade of the dopamine receptors did not significantly block or reverse the sensitizing actions of PTX, indicating that the actions of the GABAergic and dopaminergic circuits were independent. Our results thus reveal an additional, distinct inner retinal mechanism for controlling the threshold sensitivity of RGCs. It is interesting to note that activation of GABAergic circuits in the outer retina is believed to increase the sensitivity of rod bipolar cells by enhancing the effects of dopamine (Herrmann *et al.* 2011). Thus, GABAergic inhibition appears to have roles in both the inner and outer retina for controlling neuronal sensitivity. However, the effects of GABA on rod bipolar cells are clearly opposite to those described here in the inner retina. Further work is clearly called for to determine how these different mechanisms with apparently opposing actions interact to control the sensitivity of RGCs and the output signals of the retina.

Similar to the mechanism revealed in the present study, inhibitory masking of sensory afferent signals has been described throughout the CNS (Metzler & Marks, 1979; Batuev *et al.* 1982; Merzenich *et al.* 1983; Turnbull & Rasmusson, 1990; Garraghty *et al.* 1991; Jacobs & Donoghue, 1991; Gilbert & Wiesel, 1992; Faggin *et al.* 1997; Snyder *et al.* 2000; Wellman *et al.* 2002; Foeller & Feldman, 2004) and has been posited to be a component of brain plasticity in which neuronal responses are modified in changing stimulus conditions. Dynamic modulation of the masking inhibition in the retina can be a novel mechanism for neural adaptation to alter the threshold of RGCs with changes in the visual environment. For example, unmasking signals carried by the third rod pathway would be prudent at dusk or dawn because it would increase the afferent streams carrying visual information centrally. Interestingly, inhibition of rod bipolar cells is regulated by light levels, which results in a decrease of their activity in light-adapted conditions when the primary rod pathway is inactive (Eggers *et al.* 2013). Modulation of the masking inhibition may thus occur in both dim and bright ambient light conditions to limit redundant signals carried across the RGC population, which is a useful strategy to overcome the information bottleneck formed by the optic nerve.

## References


Arman AC & Sampath AP (2012). Dark-adapted response threshold of OFF ganglion cells is not set by OFF bipolar cells in the mouse retina. *J Neurophysiol* **107**, 2649–2659.

Badea TC & Nathans J (2004). Quantitative analysis of neuronal morphologies in the mouse retina visualized by using a genetically directed reporter. *J Comp Neurol* **480**, 331–351.

Balkema GW Jr & Pinto LH (1982). Electrophysiology of retinal ganglion cells in the mouse: a study of a normally pigmented mouse and a congenic hypopigmentation mutant, pearl. *J Neurophysiol* **48**, 968–980.

Batuev AS, Alexandrov AA & Scheynikov NA (1982). Picrotoxin action on the receptive fields of the cat sensorimotor cortex neurons. *J Neurosci Res* **7**, 49–55.

Baylor DA, Hodgkin AL & Lamb TD (1974). Reconstruction of the electrical responses of turtle cones to flashes and steps of light. *J Physiol* **242**, 759–791.

Beaudoin DL, Manookin MB & Demb JB (2008). Distinct expressions of contrast gain control in parallel synaptic pathways converging on a retinal ganglion cell. *J Physiol* **586**, 5487–5502.

Blakemore CB & Rushton WA (1965*a*). Dark adaptation and increment threshold in a rod monochromat. *J Physiol* **181**, 612–628.

Blakemore CB & Rushton WA (1965*b*). The rod increment threshold during dark adaptation in normal and rod monochromat. *J Physiol* **181**, 629–640.

Bloomfield SA & Miller RF (1982). A physiological and morphological study of the horizontal cell types of the rabbit retina. *J Comp Neurol* **208**, 288–303.

Boycott BB & Kolb H (1973). The connections between bipolar cells and photoreceptors in the retina of the domestic cat. *J Comp Neurol* **148**, 91–114.

Boycott BB & Wässle H (1991). Morphological classification of bipolar cells of the primate retina. *Eur J Neurosci* **3**, 1069–1088.

Cleland BG, Levick WR & Sanderson KJ (1973). Properties of sustained and transient ganglion cells in the cat retina. *J Physiol* **228**, 649–680.

Cohen E & Sterling P (1990*a*). Convergence and divergence of cones onto bipolar cells in the central area of cat retina. *Proc R Soc Lond B Biol Sci* **330**, 323–328.

Cohen E & Sterling P (1990*b*). Demonstration of cell types among cone bipolar neurons of cat retina. *Proc R Soc Lond B Biol Sci* **330**, 305–321.

Conner JD (1982). The temporal properties of rod vision. *J Physiol* **332**, 139–155.

Coombs J, van der List D, Wang GY & Chalupa LM (2006). Morphological properties of mouse retinal ganglion cells. *Neuroscience* **140**, 123–136.

Deans MR, Völgyi B, Goodenough DA, Bloomfield SA & Paul DL (2002). Connexin36 is essential for transmission of rod-mediated visual signals in the mammalian retina. *Neuron* **36**, 703–712.

Della Santina L, Inman DM, Lupien CB, Horner PJ & Wong RO (2013). Differential progression of structural and functional alterations in distinct retinal ganglion cell types in a mouse model of glaucoma. *J Neurosci* **33**, 17444–17457.

DeVries SH & Baylor DA (1995). An alternative pathway for signal flow from rod photoreceptors to ganglion cells in mammalian retina. *Proc Natl Acad Sci USA* **92**, 10658–10662.

Dowling JE & Boycott BB (1966). Organization of the primate retina: electron microscopy. *Proc Natl Acad Sci USA* **166**, 80–111.

Duan X, Qiao M, Bei F, Kim IJ, He Z & Sanes JR (2015). Subtype-specific regeneration of retinal ganglion cells following axotomy: effects of osteopontin and mTOR signaling. *Neuron* **85**, 1244–1256.

Eggers ED & Lukasiewicz PD (2010). Interneuron circuits tune inhibition in retinal bipolar cells. *J Neurophysiol* **103**, 25–37.

Eggers ED, McCall MA & Lukasiewicz PD (2007). Presynaptic inhibition differentially shapes transmission in distinct circuits in the mouse retina. *J Physiol* **582**, 569–582.

Eggers ED, Mazade RE & Klein JS (2013). Inhibition to retinal rod bipolar cells is regulated by light levels. *J Neurophysiol* **110**, 153–161.

Enz R, Brandstätter JH, Wässle H & Bormann J (1996). Immunocytochemical localization of the $GABA_C$ receptor $\rho$ subunits in the mammalian retina. *J Neurosci* **16**, 4479–4490.

Euler T & Wässle H (1995). Immunocytochemical identification of cone bipolar cells in the rat retina. *J Comp Neurol* **361**, 461–478.

Faggin BM, Nguyen KT & Nicolelis MA (1997). Immediate and simultaneous sensory reorganization at cortical and subcortical levels of the somatosensory system. *Proc Natl Acad Sci USA* **94**, 9428–9433.

Famiglietti EV Jr & Kolb H (1975). A bistratified amacrine cell and synaptic cirucitry in the inner plexiform layer of the retina. *Brain Res* **84**, 293–300.

Farrow K, Teixeira M, Szikra T, Viney TJ, Balint K, Yonehara K & Roska B (2013). Ambient illumination toggles a neuronal circuit switch in the retina and visual perception at cone threshold. *Neuron* **78**, 325–338.

Field GD & Rieke F (2002). Nonlinear signal transfer from mouse rods to bipolar cells and implications for visual sensitivity. *Neuron* **34**, 773–785.

Foeller E & Feldman DE (2004). Synaptic basis for developmental plasticity in somatosensory cortex. *Curr Opin Neurobiol* **14**, 89–95.

Fyk-Kolodziej B, Qin P & Pourcho RG (2003). Identification of a cone bipolar cell in cat retina which has input from both rod and cone photoreceptors. *J Comp Neurol* **464**, 104–113.

Garraghty PE, LaChica EA & Kaas JH (1991). Injury-induced reorganization of somatosensory cortex is accompanied by reductions in GABA staining. *Somatosens Mot Res* **8**, 347–354.

Ghosh KK, Bujan S, Haverkamp S, Feigenspan A & Wässle H (2004). Types of bipolar cells in the mouse retina. *J Comp Neurol* **469**, 70–82.

Gilbert CD & Wiesel TN (1992). Receptive field dynamics in adult primary visual cortex. *Nature* **356**, 150–152.

Hack I, Peichl L & Brandstatter JH (1999). An alternative pathway for rod signals in the rodent retina: rod photoreceptors, cone bipolar cells, and the localization of glutamate receptors. *Proc Natl Acad Sci USA* **96**, 14130–14135.

Herrmann R, Heflin SJ, Hammond T, Lee B, Wang J, Gainetdinov RR, Caron MG, Eggers ED, Frishman LJ, McCall MA & Arshavsky VY (2011). Rod vision is controlled by dopamine-dependent sensitization of rod bipolar cells by GABA. *Neuron* **72**, 101–110.

Jacobs KM & Donoghue JP (1991). Reshaping the cortical motor map by unmasking latent intracortical connections. *Science* **251**, 944–947.

Jeon CJ, Strettoi E & Masland RH (1998). The major cell populations of the mouse retina. *J Neurosci* **18**, 8936–8946.

Lee BB, Smith VC, Pokorny J & Kremers J (1997). Rod inputs to macaque ganglion cells. *Vision Res* **37**, 2813–2828.

Li L & Dowling JE (2000). Effects of dopamine depletion on visual sensitivity of zebrafish. *J Neurosci* **20**, 1893–1903.

Li P & Slaughter M (2007). Glycine receptor subunit composition alters the action of GABA antagonists. *Vis Neurosci* **24**, 513–521.

Li W, Keung JW & Massey SC (2004). Direct synaptic connections between rods and OFF cone bipolar cells in the rabbit retina. *J Comp Neurol* **474**, 1–12.

Lukasiewicz PD, Eggers ED, Sagdullaev BT & McCall MA (2004). $GABA_C$ receptor-mediated inhibition in the retina. *Vision Res* **44**, 3289–3296.

Maffei L, Fiorentini A & Cervetto L (1971). Homeostasis in retinal receptive fields. *J Neurophysiol* **34**, 579–587.

Masland RH (2012). The neuronal organization of the retina. *Neuron* **76**, 266–280.

Merzenich MM, Kaas JH, Wall JT, Sur M, Nelson RJ & Felleman DJ (1983). Progression of change following median nerve section in the cortical representation of the hand in areas 3b and 1 in adult owl and squirrel monkeys. *Neuroscience* **10**, 639–665.

Metzler J & Marks PS (1979). Functional changes in cat somatic sensory-motor cortex during short-term reversible epidural blocks. *Brain Res* **177**, 379–383.

Müller F, Wässle H & Voigt T (1988). Pharmacological modulation of the rod pathway in the cat retina. *J Neurophysiol* **59**, 1657–1672.
Muller JF & Dacheux RF (1997). Alpha ganglion cells of the rabbit retina lose antagonistic surround responses under dark adaptation. *Vis Neurosci* **14**, 395–401.
Naka KI & Rushton WA (1966). S-potentials from luminosity units in the retina of fish (Cyprinidae). *J Physiol* **185**, 587–599.
Nelson R (1977). Cat cones have rod input: a comparison of the response properties of cones and horizontal cell bodies in the retina of the cat. *J Comp Neurol* **172**, 109–135.
Pang JJ, Gao F, Lem J, Bramblett DE, Paul DL & Wu SM (2010). Direct rod input to cone BCs and direct cone input to rod BCs challenge the traditional view of mammalian BC circuitry. *Proc Natl Acad Sci USA* **107**, 395–400.
Pang JJ, Gao F & Wu SM (2003). Light-evoked excitatory and inhibitory synaptic inputs to ON and OFF $\alpha$ ganglion cells in the mouse retina. *J Neurosci* **23**, 6063–6073.
Peichl L & Wässle H (1983). The structural correlate of the receptive field centre of alpha ganglion cells in the cat retina. *J Physiol* **341**, 309–324.
Penn JS & Williams TP (1984). A new microspectrophotometric method for measuring absorbance of rat photoreceptors. *Vision Res* **24**, 1673–1676.
Pérez De Sevilla Müller L, Shelley J & Weiler R (2007). Displaced amacrine cells of the mouse retina. *J Comp Neurol* **505**, 177–189.
Petrides A & Trexler EB (2008). Differential output of the high-sensitivity rod photoreceptor: AII amacrine pathway. *J Comp Neurol* **507**, 1653–1662.
Raviola E & Gilula NB (1973). Gap junctions between photoreceptor cells in the vertebrate retina. *Proc Natl Acad Sci USA* **70**, 1677–1681.
Rodieck RW & Stone J (1965). Analysis of receptive fields of cat retinal ganglion cells. *J Neurophysiol* **28**, 832–849.
Sagdullaev BT, McCall MA & Lukasiewicz PD (2006). Presynaptic inhibition modulates spillover, creating distinct dynamic response ranges of sensory output. *Neuron* **50**, 923–935.
Sampath AP & Rieke F (2004). Selective transmission of single photon responses by saturation at the rod-to-rod bipolar synapse. *Neuron* **41**, 431–443.
Schneeweis DM & Schnapf JL (1995). Photovoltage of rods and cones in the macaque retina. *Science* **268**, 1053–1056.
Sharpe LT & Stockman A (1999). Rod pathways: the importance of seeing nothing. *Trends Neurosci* **22**, 497–504.
Snyder RL, Sinex DG, McGee JD & Walsh EW (2000). Acute spiral ganglion lesions change the tuning and tonotopic organization of cat inferior colliculus neurons. *Hear Res* **147**, 200–220.
Soucy E, Wang Y, Nirenberg S, Nathans J & Meister M (1998). A novel signaling pathway from rod photoreceptors to ganglion cells in mammalian retina. *Neuron* **21**, 481–493.
Stone C & Pinto LH (1993). Response properties of ganglion cells in the isolated mouse retina. *Vis Neurosci* **10**, 31–39.
Strettoi E, Dacheux RF & Raviola E (1990). Synaptic connections of rod bipolar cells in the inner plexiform layer of the rabbit retina. *J Comp Neurol* **295**, 449–466.
Sun W, Li N & He S (2002). Large-scale morphological survey of mouse retinal ganglion cells. *J Comp Neurol* **451**, 115–126.
Thibos LN & Werblin FS (1978). The properties of surround antagonism elicited by spinning windmill patterns in the mudpuppy retina. *J Physiol* **278**, 101–116.
Tsukamoto Y, Morigiwa K, Ishii M, Takao M, Iwatsuki K, Nakanishi S & Fukuda Y (2007). A novel connection between rods and ON cone bipolar cells revealed by ectopic metabotropic glutamate receptor 7 (mGluR7) in mGluR6-deficient mouse retinas. *J Neurosci* **27**, 6261–6267.
Tsukamoto Y, Morigiwa K, Ueda M & Sterling P (2001). Microcircuits for night vision in mouse retina. *J Neurosci* **21**, 8616–8623.
Turnbull BG & Rasmusson DD (1990). Acute effects of total or partial digit denervation on raccoon somatosensory cortex. *Somatosens Mot Res* **7**, 365–389.
Veruki ML & Hartveit E (2002). Electrical synapses mediate signal transmission in the rod pathway of the mammalian retina. *J Neurosci* **22**, 10558–10566.
Völgyi B, Chheda S & Bloomfield SA (2009). Tracer coupling patterns of the ganglion cell subtypes in the mouse retina. *J Comp Neurol* **512**, 664–687.
Völgyi B, Deans MR, Paul DL & Bloomfield SA (2004). Convergence and segregation of the multiple rod pathways in mammalian retina. *J Neurosci* **24**, 11182–11192.
Wang P & Slaughter MM (2005). Effects of GABA receptor antagonists on retinal glycine receptors and on homomeric glycine receptor alpha subunits. *J Neurophysiol* **93**, 3120–3126.
Wässle H, Koulen P, Brandstatter JH, Fletcher EL & Becker CM (1998). Glycine and GABA receptors in the mammalian retina. *Vision Res* **38**, 1411–1430.
Wellman CL, Arnold LL, Garman EE & Garraghty PE (2002). Acute reductions in $GABA_A$ receptor binding in layer IV of adult primate somatosensory cortex after peripheral nerve injury. *Brain Res* **954**, 68–72.
Zhou C & Dacheux RF (2005). Glycine- and GABA-activated inhibitory currents on axon terminals of rabbit cone bipolar cells. *Vis Neurosci* **22**, 759–767.

## Additional information

### Competing interests

None declared.

### Author contributions

F.P. and S.A.B.: conception and design of the work. F.P., A.T., Y.Z., T.A., H.R., K.R., B.V., A.A. and S.A.B.: acquisition, analysis and

interpretation of data. F.P., A.A. and S.A.B.: drafting the article. All authors approved the final version of this manuscript and agree to be accountable for all aspects of the work in ensuring that questions related to the accuracy or integrity of any part of the work are appropriately investigated and resolved. All persons designated as authors qualify for authorship, and all those who qualify for authorship are listed.

## Funding

This study was supported by National Institutes of Health grant EY007360 awarded to S.A.B.

## Acknowledgements

We thank Kevin Chen for help with data analyses.